Multiple mechanisms link prestimulus neural oscillations to sensory responses

Luca Iemi[1,2,3], Niko A Busch[4,5], Annamaria Laudini[6], Jason Samaha[7], Arno Villringer[3,6], and Vadim V Nikulin[2,3]

[1] *Dept of Neurological Surgery, Columbia University Medical Center, New York, NY 10032, USA*
[2] *Center for Cognition and Decision Making, National Research University Higher School of Economics, Myasnitskaya ulitsa, 20, 101000, Moscow, Russian Federation*
[3] *Department of Neurology, Max Planck Institute for Human Cognitive and Brain Sciences, Stephanstr. 1a, 04103 Leipzig, Germany*
[4] *Institute of Psychology, University of Münster, Fliednerstr. 21, 48149 , Münster, Germany*
[5] *Otto Creutzfeldt Center for Cognitive and Behavioral Neuroscience, University of Münster, Germany*
[6] *Berlin School of Mind and Brain, Humboldt-Universität zu Berlin, Unter den Linden 6, 10099 Berlin, Germany*
[7] *Department of Psychology, University of California, Santa Cruz, Santa Cruz, CA, USA*

Acknowledgments
This work was supported by the HSE Basic Research Program and the Russian Academic Excellence Project '5-100' (LI, VVN), and by a grant from the German Research Foundation (DFG) to NAB (BU2400/9-1).

We thank Francesco Di Russo and Volodymyr B Bogdanov for help with designing the stimuli, Johanna Rehder for help with the literature search, and Charles Schroeder, Saskia Haegens, and Omri Raccah for comments on the manuscript.

Abstract

Why do brain responses (e.g. event-related potentials, ERPs) vary across repeated presentations of the same stimulus? Fluctuations in neural excitability, indexed by prestimulus oscillations (8—30 Hz), are hypothesized to account for this variability. In this study, we considered different mechanisms for ERP generation and how they may be modulated by prestimulus oscillations. During stimulation with identical visual stimuli, we found that strong prestimulus alpha- and beta-band power inhibit sensory responses as characterized by early ERP components (C1 and N150). In addition, we confirmed that the late component of the ERP was generated by a baseline shift due to the event-related modulation of non-zero-mean oscillations. Importantly, we found that strong prestimulus power lead to greater event-related desynchronization (ERD), which manifested as an amplified late ERP component. Our results reveal that at least two distinct mechanisms give rise to the relationship between prestimulus brain activity and sensory responses.

Introduction

The amplitude of event-related potentials (ERPs) varies across repeated presentations of the same sensory stimulus (Arieli et al., 1996; Truccolo et al., 2002; De Munck et al., 2004). This response variability might be accounted for by spontaneous fluctuations of prestimulus brain states, partly reflected by the power of low-frequency oscillations (8–30 Hz). Previous studies on the effect of prestimulus power on the ERP amplitude have been inconsistent regarding the latency and even the directionality of this modulatory effect. Specifically, several studies found that prestimulus α-band power suppresses the amplitude of early ERP components ($<$ 0.200 s: Rahn and Başar, 1993; Roberts et al., 2014; Becker et al., 2008; Başar and Stampfer, 1985; Jasiukaitis and Hakerem, 1988), whereas other studies found that prestimulus α-band power amplifies the amplitude of late ERP components ($>$ 0.200 s: Dockree et al., 2007; Becker et al., 2008; Roberts et al., 2014; Başar and Stampfer, 1985; Jasiukaitis and Hakerem, 1988; Barry et al., 2000). To date, the underlying mechanism of these modulatory effects remains elusive. In this study, we addressed this issue by considering how prestimulus power modulates the mechanisms of ERP generation at different latencies.

ERP components occurring during the early time window ($<$ 0.200 s) are thought to be generated by an activation of sensory brain areas adding on top of ongoing activity (additive mechanism; Bijma et al., 2003; Shah et al., 2004; Mäkinen et al., 2005; Mazaheri and Jensen, 2006). Invasive studies in non-human primates demonstrated that early ERP components are associated with an increase in the magnitude of multi-unit activity (MUA) in sensory areas (Kraut et al., 1985; Schroeder et al., 1990, 1991; Schroeder, 1998; Shah et al., 2004; Lakatos et al., 2007), presumably as a result of membrane depolarization due to excitatory synaptic activation (Schroeder et al., 1995). Non-invasive studies in humans showed that early ERP components (e.g., C1) are associated with an increase in the hemodynamic fMRI signal in visual areas (Di Russo et al., 2001, 2003), which may reflect an additive sensory response. Low-frequency neural oscillations are thought to set the state of the neural system for information processing (Jensen and Mazaheri, 2010; Mathewson et al., 2011; Spitzer and Haegens, 2017), which in turn may modulate the generation of additive ERP components. In particular, numerous studies have demonstrated that states of strong ongoing α- and β-band oscillations reflect a state of functional inhibition, indexed by a reduction of neuronal excitability (e.g., single-unit activity: Haegens et al., 2011; Watson et al., 2018; MUA: van Kerkoerle et al., 2014; Becker et al., 2015; ongoing γ-band power: Spaak et al., 2012; hemodynamic fMRI signal: Goldman et al., 2002; Becker et al., 2011; Scheeringa et al., 2011; Harvey et al., 2013; Mayhew et al., 2013) and of subjective perception (e.g., conservative perceptual bias: Limbach and Corballis, 2016; Iemi et al., 2017; Craddock et al., 2016; Iemi and

Busch, 2018; lower perceptual confidence: Samaha et al., 2017b; lower visibility ratings: Benwell et al., 2017b). Accordingly, prestimulus low-frequency oscillations may exert an inhibitory effect on the additive mechanism of ERP generation: i.e., states of strong prestimulus power may suppress the activation of sensory areas, resulting in an attenuation of the amplitude of additive ERP components, primarily generated during the early time window (Fig 1).

While early ERP components are likely to be generated primarily through an additive mechanism, late ERP components can have a contribution from both additive and baseline shift mechanisms (where "baseline" denotes the mean offset of the signal, rather than prestimulus activity). According to the baseline shift mechanism, the slow ERP component, which becomes visible during the late time window (> 0.200 s), is thought to be generated by a modulation of ongoing oscillatory power, rather than by an additive response (Nikulin et al., 2007, 2010a; Mazaheri and Jensen, 2008, 2010; Dijk et al., 2010). The effect of the baseline shift mechanism on the relationship between prestimulus power and ERP amplitude has never been tested. In fact, it is generally assumed (and not even questioned) that neural oscillations are symmetrical around the zero line of the signal. Accordingly, trial averaging is expected to eliminate non-phase-locked oscillations due to phase cancellation (assuming a random phase distribution over trials), thereby resulting in a signal baseline with a zero mean. It follows that a modulation of zero-mean oscillations by stimuli/tasks leaves the signal baseline unaffected (Fig 1 A).

In contrast to this traditional view, recent studies (Nikulin et al., 2007, 2010a; Mazaheri and Jensen, 2008; Dijk et al., 2010; Schalk, 2015; Cole and Voytek, 2016) proposed that neural oscillations do not vary symmetrically around the zero line of the signal, but rather around a non-zero offset/mean (Fig 1 B).Accordingly, trial averaging does not eliminate non-phase-locked oscillations with a non-zero mean. As a consequence, any amplitude modulation of oscillations with a non-zero mean is expected to change the signal baseline (baseline shift), and thus will affect the ERP amplitude. Specifically, during the event-related desynchronization (ERD) of low-frequency oscillations, the power suppression is expected to cause a slow shift of the signal baseline toward the zero line. Subtracting the prestimulus non-zero baseline from the post-stimulus signal creates a slow shift, which mirrors the spatio-temporal profile of the ERD. In particular, an ERD of oscillations with a negative non-zero-mean is expected to generate an upward slow shift of the ERP (and viceversa). The idea that the ERD contributes to the generation of the slow ERP component, implies that the larger the ERD, the stronger the slow ERP component. Accordingly, we predicted that states of strong prestimulus power would yield a strong ERD (Becker et al., 2008; Tenke et al., 2015; Benwell et al., 2017a), resulting in an enhancement of the slow ERP component visible during the late time window.

To summarize, states of strong prestimulus power are expected: i) to suppress the amplitude of ERP components during the early time window, generated by a stimulus-evoked activation (via functional inhibition); and ii) to amplify the late ERP component, generated by a stimulus-induced modulation of non-zero-mean oscillations (via baseline shift). To test these predictions, we recorded electroencephalography (EEG) in human participants during rest and during stimulation with identical high-contrast checkerboard stimuli and analyzed the relationship between ERPs, ongoing and event-related oscillations. To anticipate, the effects of prestimulus power on early and late ERP components are consistent with the functional inhibition and baseline shift mechanisms, respectively. Taken together, these results largely resolve apparent inconsistencies in previous literature and specify two distinct mechanisms by which prestimulus neural oscillations modulate visual ERP components.

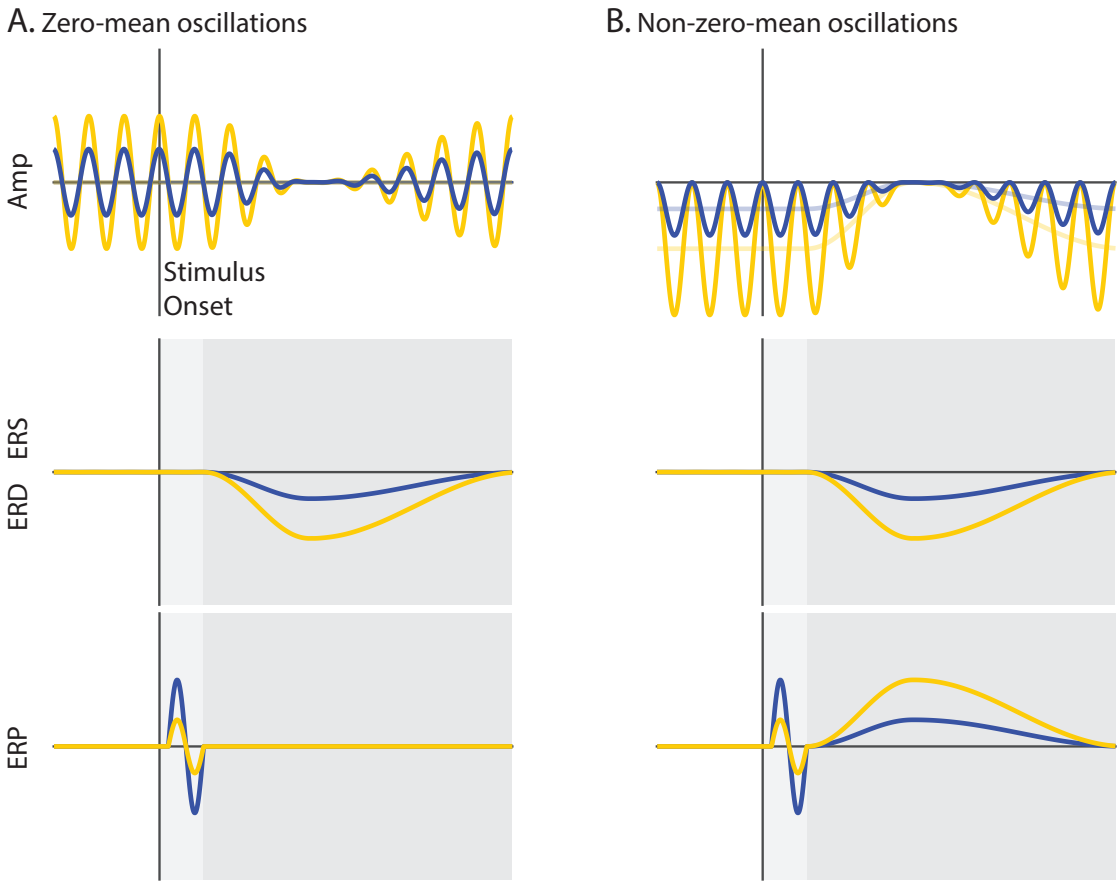

Figure 1: Schematic overview of the mechanisms of functional inhibition and baseline shift. Ongoing activity (Amplitude), event-related oscillations (ERD/ERD) and potentials (ERP) are illustrated in rows 1, 2, 3, respectively. The vertical line indicates stimulus onset, while the horizontal line indicates zero. Yellow and blue represent states of strong and weak prestimulus power, respectively. **A**: Non-phase-locked ongoing oscillatory activity with a zero-mean. The oscillations are symmetrical relative to the zero line of the signal (row 1). **B**: Non-phase-locked ongoing oscillatory activity with a non-zero-mean. The oscillations are asymmetrical relative to the zero line of the signal. The signal baseline is characterized by a negative offset (opaque lines). The stronger the power of these oscillations, the stronger the negative offset of the signal baseline (row 1). During event-related desynchronization (ERD), the ongoing oscillations are suppressed to the zero line of the signal. This implies that the stronger the prestimulus power, the stronger the ERD (row 2). Trial averaging of zero-mean oscillations eliminates prestimulus oscillatory activity that is not time-locked to the stimulus because opposite oscillatory phases cancel out. This results in baseline signal at the zero line, which is unaffected by the ERD. Therefore, an ERD of zero-mean oscillations does not generate the slow ERP component during the late time window because there is no baseline shift for these oscillations (column A, row 3). Trial averaging of non-zero-mean oscillations does not eliminate non-phase locked ongoing activity. This results in a prestimulus baseline signal with an offset relative to the zero line. During the ERD, the baseline of the signal gradually goes to the zero line of the signal. When the post-stimulus signal is corrected with the prestimulus non-zero baseline, a slow shift of the ERP signal appears, mirroring the ERD time-course. Specifically, an ERD of negative (positive) non-zero mean oscillations shifts the signal upward (downward), generating the slow ERP component of positive (negative) polarity. Crucially, the stronger the prestimulus power, the stronger the ERD, and as a consequence, the stronger the slow shift of the ERP. The baseline shift mechanism predicts a positive relationship between prestimulus power and the amplitude of the slow ERP during the late time window (dark gray) (column B, row 3). According to the functional inhibition mechanism, strong prestimulus power attenuates the amplitude of the additive ERP components. This mechanism predicts a negative relationship between prestimulus power and the amplitude of ERP components during the early time window (light gray) (row 3).

Results

Event-related potentials

The experiment included stimulation trials with high-contrast checkerboard stimuli presented in the lower (LVF; Fig 2 A, column 1) or upper (UVF; Fig 2 A, column 2) visual field with equal probability, and fixation-only trials without any checkerboard stimulus (F; Fig 2 A, column 3). All trials included a change of the central fixation mark at the time of stimulus presentation (see Methods for details). For each participant we quantified the ERP at the electrode with peak activity between 0.055 and 0.090 s after stimulus onset, reflecting the C1 component which indicates initial afferent activity in primary visual cortex (Di Russo et al., 2001).

In stimulation trials, the C1 component peaked on average at 0.079 s (SEM = 0.001) and at 0.078 s (SEM = 0.001) for LVF and UVF stimuli respectively, with a maximum at occipito-parietal electrodes (Fig 2 B, column 1 and 2). The comparison of C1 amplitudes at individual peak electrodes on LVF (M = 10.157 μV ; SEM = 0.918) and UVF (M= -10.567 μV; SEM = 1.058) trials revealed the expected polarity reversal, confirming that this component originates from initial afferent activity in early visual areas (Di Russo et al., 2001, 2003; Bao et al., 2010). Following the C1, we observed a N150 component peaking between 0.100 and 0.200 s relative to stimulus onset, with an occipital topography and a consistently negative polarity for both LVF and UVF stimuli. The N150 was followed by a late deflection in the time range between 0.200 and 0.600 s relative to stimulus onset, with a parietal topography and consistent positive polarity for both LVF and UVF stimuli.

As expected, in F trials no C1 component was detected in the ERP at individual C1-peak electrodes for LVF and UVF stimuli (mean amplitude in the C1 time window: -0.044 μV, SEM = 0.196). F trials showed a late positive deflection with similar timing and topography as in stimulation trials (Fig 2 B, column 3).

Event-related oscillations

For each participant we estimated the event-related synchronization (ERS) and desynchronization (ERD) at frequencies between 5 and 30 Hz and at each electrode and time point of the post-stimulus window (0–0.900 s). For the group-level statistical analysis, we used cluster permutation test to determine at which time, frequency and electrode the ERS/ERD was significantly different from 0 across participants. For LVF stimulation trials, the statistical test revealed a negative cluster ($p < 0.001$) indicating ERD, spanning time points from 0 to 0.900 s relative to stimulus onset, frequencies between 6 and 30 Hz, and all 64 electrodes (Fig 2 C, column 1). The maximum negative t statistic was found at 20 Hz, 0.234 s, and at electrode P7. A positive cluster ($p = 0.041$) indicating ERS spanned time points from 0 to 0.900 s relative to stimulus onset, frequencies between 5 and 8 Hz, and all 64 electrodes. The maximum positive t statistic was found at 5 Hz, 0.097 s, and at electrode P7.

For UVF stimulation trials, the statistical test revealed a negative cluster ($p < 0.001$) indicating ERD, spanning time points from 0 to 0.900 s relative to stimulus onset, frequencies between 6 and 30 Hz, and all 64 electrodes (Fig 2 C, column 2). The maximum negative t statistic was found at 20 Hz, 0.234 s, and at electrode P7. The statistical test also found two positive clusters indicating ERS. The first positive cluster ($p = 0.032$) spanned time points from 0 to 0.900 s relative to stimulus onset, frequencies between 5 and 8 Hz, and all 64 electrodes. Within this cluster, the maximum positive t statistic was found at 5 Hz, 0.152 s, and at electrode P2. The

second positive cluster ($p = 0.034$) spanned time points from 0.49 to 0.900 s relative to stimulus onset, frequencies between 13 and 30 Hz, and 62 electrodes. Within this cluster, the maximum positive t statistic was found at 17 Hz, 0.648 s, and at electrode FT7.

For F trials, the cluster permutation test revealed one negative cluster ($p < 0.001$) indicating ERD, spanning time points from 0 to 0.900 s relative to stimulus onset, frequencies between 5 and 30 Hz, and all 64 electrodes (Fig 2 C, column 3). Note that "stimulus onset" in F trials refers to the time when a C1-eliciting stimulus would be presented in stimulation trials (see Methods for details). In F trials, the maximum t statistic was found at 20 Hz, 0.214 s, and at electrode PO8.

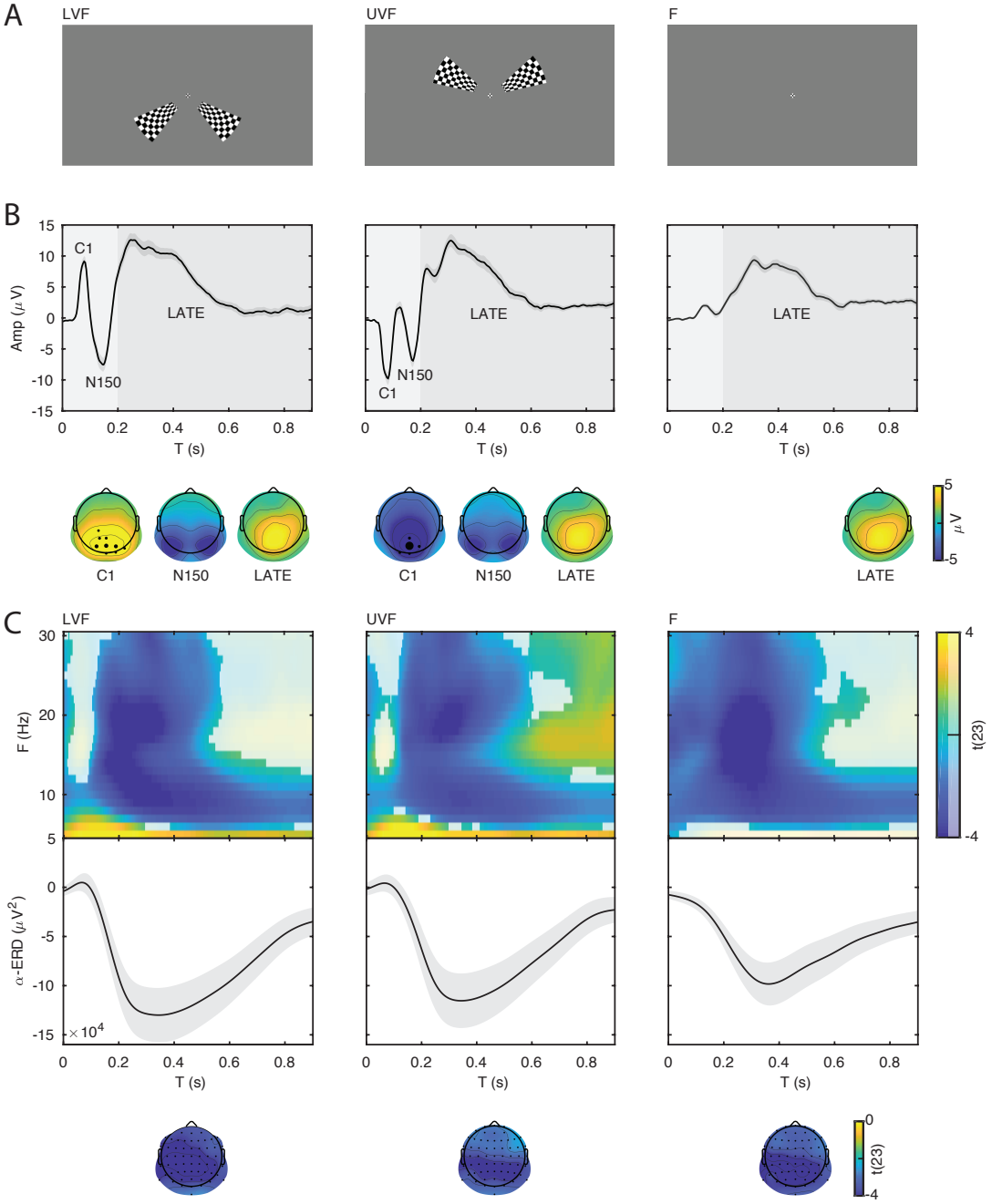

Figure 2: Event-related potentials and oscillations. **A**: The stimuli consisted in bilateral checkerboard wedges specifically designed to elicit the C1 component of the visual ERP. The stimuli appeared in the lower (column 1, LVF), upper visual field (column 2, UVF), or in no field (column 3, F) with equal probability. Across trials, the participants were instructed to discriminate a central target during stimulus presentation. **B**: Event-related potentials (ERP) were calculated for the subject-specific electrode with C1-peak activity. Additive ERP components are visible during the early time window (< 0.200 s, light grey). The C1 component is the earliest component of the visual ERP and is polarity-reversed across fields of stimulation (LVF vs. UVF). The C1 topography illustrates the ERP amplitude averaged at the subject-specific time point of peak activity between 0.055 and 0.090 s. The size of the electrodes in the topography indicate the frequency of the C1-peak electrode in the sample of participants. The C1 is followed by N150, peaking between 0.130 and 0.180 s relative to stimulus onset. The N150 topography illustrates the ERP amplitude averaged between 0.130 and 0.180 s. F trials do not show any robust additive components during the early time window.(continue next page)

Figure 2: (Previous page.) The slow component of the ERP is visible during the late time window ($>$ 0.200 s, dark gray). The topography of this late component illustrates the ERP amplitude averaged between 0.200 and 0.900 s. This late ERP component is present in all trial types. Time 0 indicates stimulus onset. **C**: Group-level t statistics map of event-related oscillations. Negative values (blue) indicate significant power suppression across participants (ERD), while positive values (yellow) indicate significant power enhancement across participants (ERS). The map is averaged across electrodes of the significant clusters. The maps are masked by a p value of 0.05 using two-sided cluster permutation testing. The topography illustrates the group-level t-statistics averaged for the α frequency band (8–12 Hz) at the time point of minimum t statistics. The bottom insets illustrate the group-level α-band ERD time course at occipital electrodes. The ERD is present in all trial types. Time 0 s indicates stimulus onset. Column 1, 2, and 3 show the results in lower visual field (LVF), upper visual field (UVF) and fixation-only (F) trials, respectively.

Evidence for functional inhibition

The functional inhibition mechanism predicts that states of strong prestimulus power reflect neural inhibition, resulting in reduced amplitudes specifically of early ERP components generated in early sensory areas by an additive mechanism.

For LVF stimulation trials, a statistical test comparing ERP amplitudes during the early time window ($<$ 0.200 s) on trials with strong versus weak prestimulus power found a significant negative cluster ($p = 0.015$). This indicates that the ERP amplitude in a time range containing the C1 (0.043 to 0.121 s) was weaker (i.e. less positive) on trials with strong prestimulus power between 8 and 28 Hz, and at all 64 electrodes (Fig 3 A, column 1). The maximum t statistic was found at 10 Hz, 0.078 s, and at electrode P4. Furthermore, the statistical test found a significant positive cluster ($p < 0.001$), indicating that the ERP amplitude in a time range containing with the N150 (0.090 to 0.200 s) was weaker on trials with strong prestimulus power between 5 and 24 Hz, and at all 64 electrodes (Fig 3 A, column 1). The maximum t statistic was found at 9 Hz, 0.098 ms, and at electrode Pz.

For UVF stimulation trials, the statistical test during the early time window found two significant positive clusters. The first cluster ($p < 0.001$) indicated that the ERP amplitude in a time range containing the C1 (0.02 to 0.113 s) was weaker (i.e. less negative) on trials with strong prestimulus power between 5 and 22 Hz, and at all 64 electrodes (Fig 3 A, column 2). The maximum t statistic was found at 13 Hz, 0.082 ms, and at electrode PO4. The second cluster indicated that the ERP amplitude in a time range containing the N150 (0.125 to 0.200 s) was weaker on trials with strong prestimulus power between 5 and 25 Hz, and at all 64 electrodes. The maximum t statistic was found at 10 Hz, 0.177 ms, and at electrode F2.

For F trials, the statistical test during the early time window found no significant clusters ($<$ 0.200 s, Fig 3 A, column 3).

Taken together, the results on early ERP components show that ERP amplitude in stimulation trials is attenuated during states of strong prestimulus power, regardless of the polarity of the components. This provides evidence for the functional inhibition mechanism underlying the modulatory effect of prestimulus power on the early ERP components.

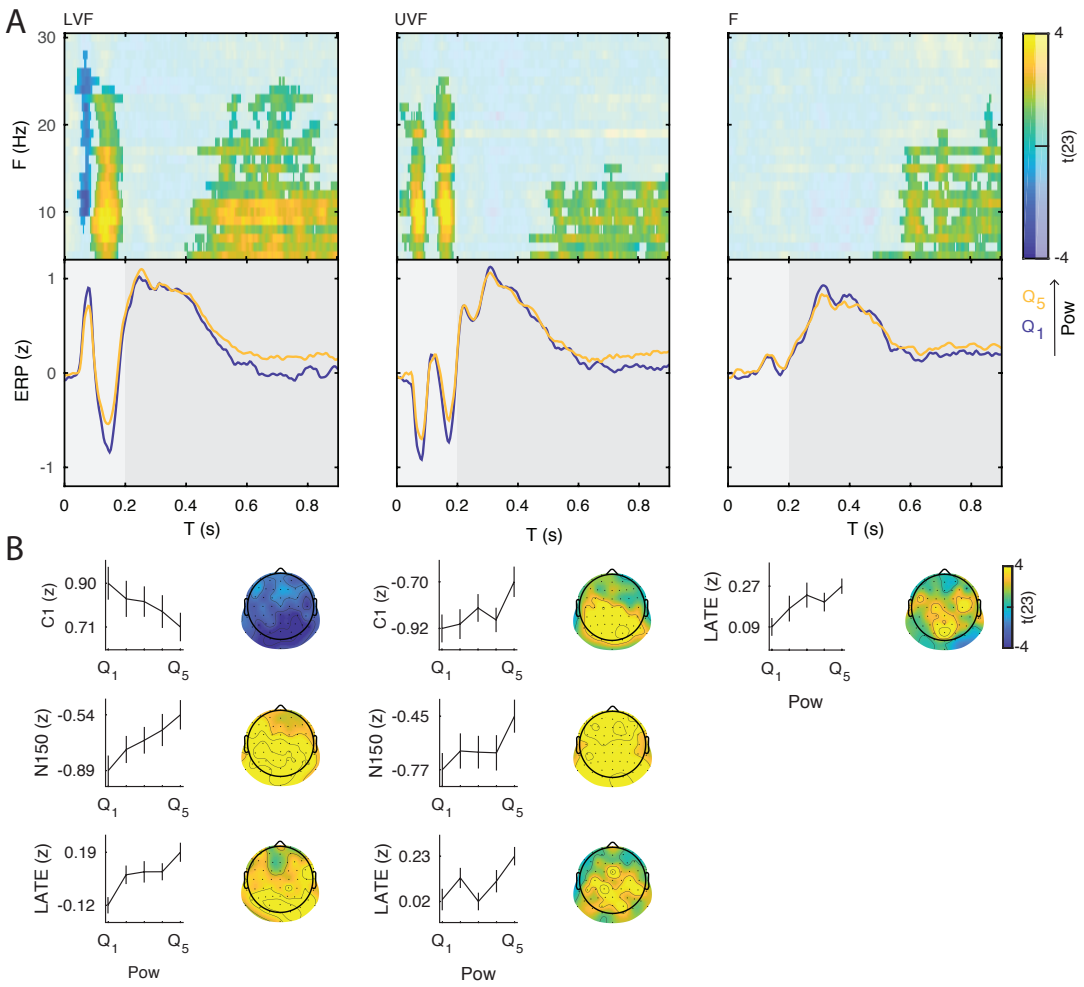

Figure 3: Prestimulus power differently modulates the amplitude of early and late event-related potentials (ERP). **A**: Group-level t statistics map of the difference in ERP amplitude between states of weak (Q_1) and strong (Q_5) prestimulus power for lower visual field stimuli (column 1, LVF), upper visual field stimuli (column 2, UVF), and in fixation-only trials (column 3, F). Positive (yellow) and negative values (blue) indicate that ERP amplitude increases and decreases during states of strong prestimulus power, respectively. The map is averaged across electrodes of the significant cluster. The maps are masked by a p value of 0.025 using separate two-sided cluster permutation testing for early and late time windows. Note that the x axis refers to post-stimulus ERP time, while the y axis refers to the frequency of prestimulus oscillatory power. Bottom insets: visualization of the normalized ERP time course separately for states of strong (Q_5, yellow) and weak (Q_1, blue) prestimulus power. This was computed at the electrode and frequency of minimum/maximum t-statistics during the C1 time window in stimulation trials and during the late time window in F trials. The ERP is characterized by distinct components occurring during the early ($<$ 0.200 s: C1 and N150, light gray) and late time window ($>$ 0.200 s, dark gray). Time 0 indicates stimulus onset. **B**: Group-average normalized ERP amplitude in trials sorted from weak (Q_1) to strong (Q_5) prestimulus power, calculated at the ERP time point and the prestimulus-power electrode and frequency of minimum/maximum t-statistics. Error bars indicate $\pm$SEM. The topography show the positive and negative t statistics at the at the time point and frequency of minimum/maximum t-statistic for early (C1 and N150) and late ERP components. Black dots represent electrodes comprising the significant clusters. States of strong prestimulus power are followed by a reduction of the amplitude of additive ERP components during the early time window (consistent with the functional inhibition mechanism), as well as by an enhancement of the slow ERP component during the late time window (consistent with the baseline shift mechanism).

Evidence for the baseline shift mechanism

The baseline shift mechanism predicts that states of strong prestimulus oscillations with a non-zero mean are followed by strong post-stimulus power suppression (ERD), resulting in greater ERP amplitudes specifically during the late time window. To demonstrate that the late ERP component was generated by a baseline shift, it is necessary to establish that: i) the ongoing oscillations have a non-zero mean; ii) the non-zero mean and the late ERP component have opposite polarity; and that iii) the ERD magnitude is associated with the amplitude of the late ERP component.

To demonstrate the non-zero mean property of ongoing oscillations, we computed the Baseline Shift Index (BSI: Nikulin et al., 2007, 2010a) and the Amplitude Fluctuation Asymmetry Index ($AFAI$: Mazaheri and Jensen, 2008). For each participant we estimated BSI and $AFAI$ from resting-state oscillations for each electrode and frequency between 5 and 30 Hz, and then tested whether these indexes were significantly different from 0 across participants using a cluster permutation test.For $AFAI$, we found a significant negative cluster (p-value $<$ 0.001) between 5 and 30 Hz with a parietal, occipital and central topography (Fig 4 A/B), indicating a stronger modulation of the troughs relative to the peaks, resulting in a negative mean. For BSI, we found a significant negative cluster (p-value $<$ 0.001) between 5 and 21 Hz with a parietal, occipital and central topography (Fig 4 A/B), similar to $AFAI$. BSI $<$ 0 indicates that strong oscillatory power corresponds to a more negative value of the low-pass filtered signal, as expected in the presence of oscillations with a negative mean. Taken together, the results on BSI and $AFAI$ provide evidence for a non-zero (negative) mean of resting-state low-frequency oscillations. It is important to note that the late ERP component had a positive polarity in all trial types (Fig 1), which is expected as a result of ERD of oscillations with a negative mean (Nikulin et al., 2007, 2010a; Mazaheri and Jensen, 2008).

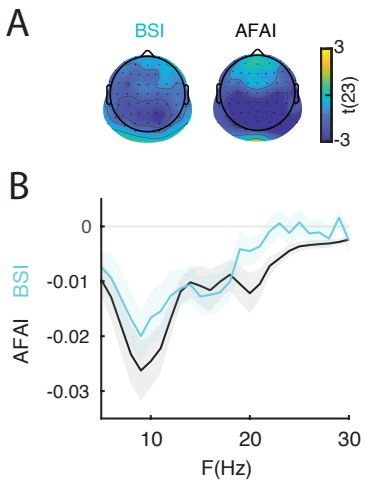

Figure 4: The non-zero mean property of resting-state neural oscillations. One prerequisite for the baseline shift mechanism is that the oscillations have a non-zero mean. The late component of the ERP is generated by a baseline shift occurring during event-related desynchronization (ERD) of non-zero mean oscillations. **A**: The amplitude fluctuation asymmetry index ($AFAI$) is quantified as the normalized difference between the variance of the peaks and troughs of an oscillatory signal during resting-state. $AFAI < 0$ (blue) indicates a stronger modulation of the troughs relative to the peaks, consistent with a negative mean. The topography represents the group-level t-statistics of $AFAI$: a significant negative cluster was found at frequencies between 5 and 30 Hz and with an occipito-parietal peak. The baseline shift index (BSI) is quantified as the correlation between the oscillatory envelope at a certain frequency and low-pass filtered EEG signal at 3 Hz during resting-state. $BSI < 0$ (blue) indicate a negative relationship between oscillatory envelope and low-pass filtered signal, consistent with negative mean. The topography represents the group-level t-statistics of BSI: a significant negative cluster was found at frequencies between 5 and 21 Hz and with an occipito-parietal peak. Black dots represent electrodes comprising the significant clusters. **B**: Comparison between group-level $AFAI$ (black) and BSI (blue), averaged across respective cluster electrodes, and shown for each frequency. Shaded areas indicate $\pm$SEM. These results indicate the presence of a negative oscillatory mean, consistent with the baseline shift mechanism.

Next, we analyzed the relationship between the ERD magnitude and the ERP amplitude during the late time window ($>$ 0.200 s). We compared the amplitude of the late ERP between groups of trials of weak and strong ERD estimated at each frequency and electrode. For the group-level statistical analysis, we used cluster permutation test to determine significant ERP differences across ERP time points, and ERD electrodes and frequencies. The statistical test in LVF stimulation trials revealed one significant positive cluster ($p < 0.001$), indicating that the late ERP (0.200–0.900 s) was greater during states of stronger ERD at frequencies between 5 and 30 Hz, and at all 64 electrodes (Fig 5 A/B, column 1). The maximum t statistic was found at 8 Hz, 0.266 s, and at electrode POz. The statistical test in UVF stimulation trials revealed two significant positive clusters, indicated that the late ERP (cluster 1: 0.336–0.900 s; cluster 2: 0.200 to 0.328) was greater during states of strong ERD at frequencies between 5 and 30 Hz, and at all 64 electrodes (Fig 5 A/B, column 2). The maximum t statistic was found at 19 Hz, 0.258 s, and at T8 electrode. The statistical test in F trials revealed one significant positive cluster ($p < 0.001$), indicating that the late ERP (0.488–0.900 s) was greater during states of strong ERD at frequencies between 5 and 30 Hz, and at all 64 electrodes (Fig 5 A/B, column 3). The maximum t statistic value was found at 13 Hz, 0.637 s, and at electrode PO8.

Taken together, these results indicate that states of stronger ERD were associated with a more positive deflection of the late ERP component, consistent with the baseline shift mechanism.

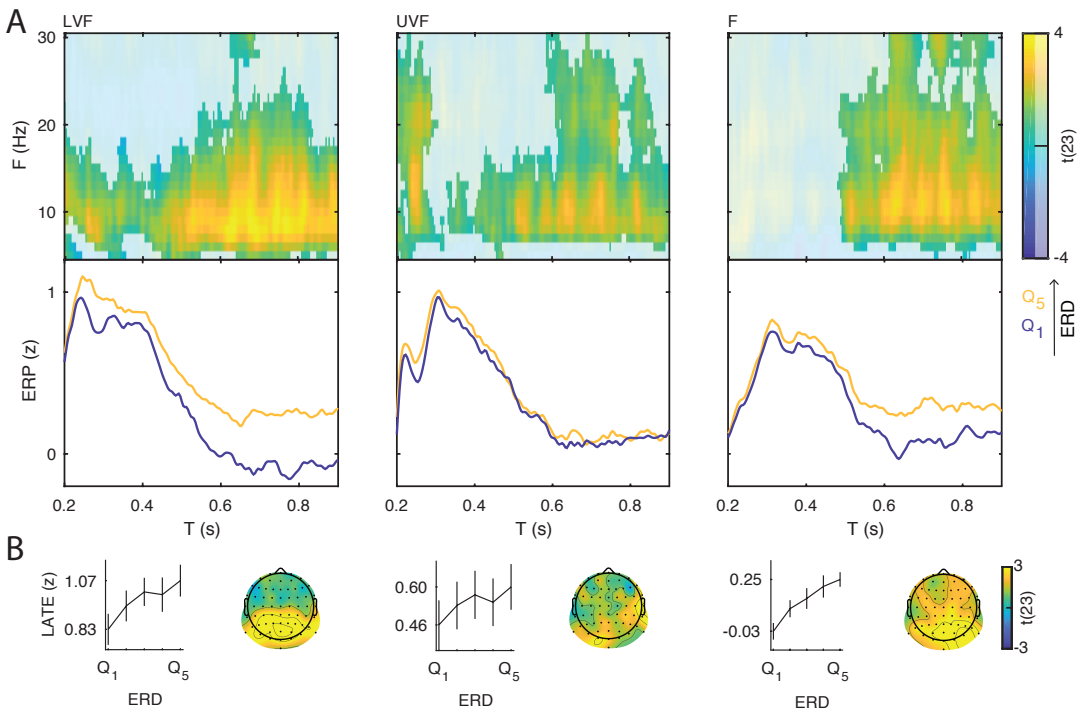

Figure 5: Interaction between the event-related desynchronization (ERD) and the late ERP component. A positive relationship between the ERD magnitude and the late ERP amplitude is another prerequisite for the baseline shift mechanism. **A**: Group-level t statistics map of the difference in late ERP amplitude ($>$ 0.200 s) between states of weak (Q_1) and strong (Q_5) event-related desynchronization (ERD) for lower visual field stimuli (column 1), upper visual field stimuli (column 2), and in fixation-only trials (column 3). Positive values (yellow) indicate that the amplitude of the late ERP increases during states of strong ERD. The map is averaged across electrodes of the significant cluster. The maps are masked by a p value of 0.05 using two-sided cluster permutation testing. Note that the x axis refers to post-stimulus ERP time, while the y axis refers to the ERD frequency. Bottom insets: visualization of the normalized late ERP time course separately for states of strong (Q_5, yellow) and weak (Q_1, blue) ERD, computed at the electrode and frequency of maximum t-statistics. Time 0 indicates stimulus onset. **B**: Group-average normalized ERP amplitude in trials sorted from weak (Q_1) to strong (Q_5) ERD, calculated at the ERP time point and ERD electrode and frequency of maximum t-statistics. The amplitude of the late ERP increases linearly as a function of ERD. Error bars indicate $\pm$SEM. The topographies show the positive t statistics of the significant clusters at the at the time point and frequency of maximum t-statistics for each trial type. Black dots represent electrodes comprising the significant positive cluster. Taken together, these results show that states of strong ERD are associated with an enhancement of the late ERP component, consistent with the baseline shift mechanism.

After demonstrating that the ERD magnitude correlates with the late ERP amplitude, we tested whether the ERD magnitude was, in turn, correlated with prestimulus power. To this end, we compared the ERD magnitude (at the subject-specific C1 electrode) between groups of trials of weak and strong prestimulus power estimated for each frequency and electrode. For the group-level statistical analysis, we used a cluster permutation test to determine significant differences across ERD time points, prestimulus-power frequencies, and electrodes.

The statistical test revealed a large significant cluster in each trial type ($p < 0.001$), spanning frequencies between 5 and 30 Hz, time points between 0 and 0.900 s, and all 64 electrodes (Fig 6: LVF trials in A, column 1; UVF trials in A, column 2; and F trials in A, column 3), indicating that at low frequencies strong prestimulus oscillations were associated with strong ERD.

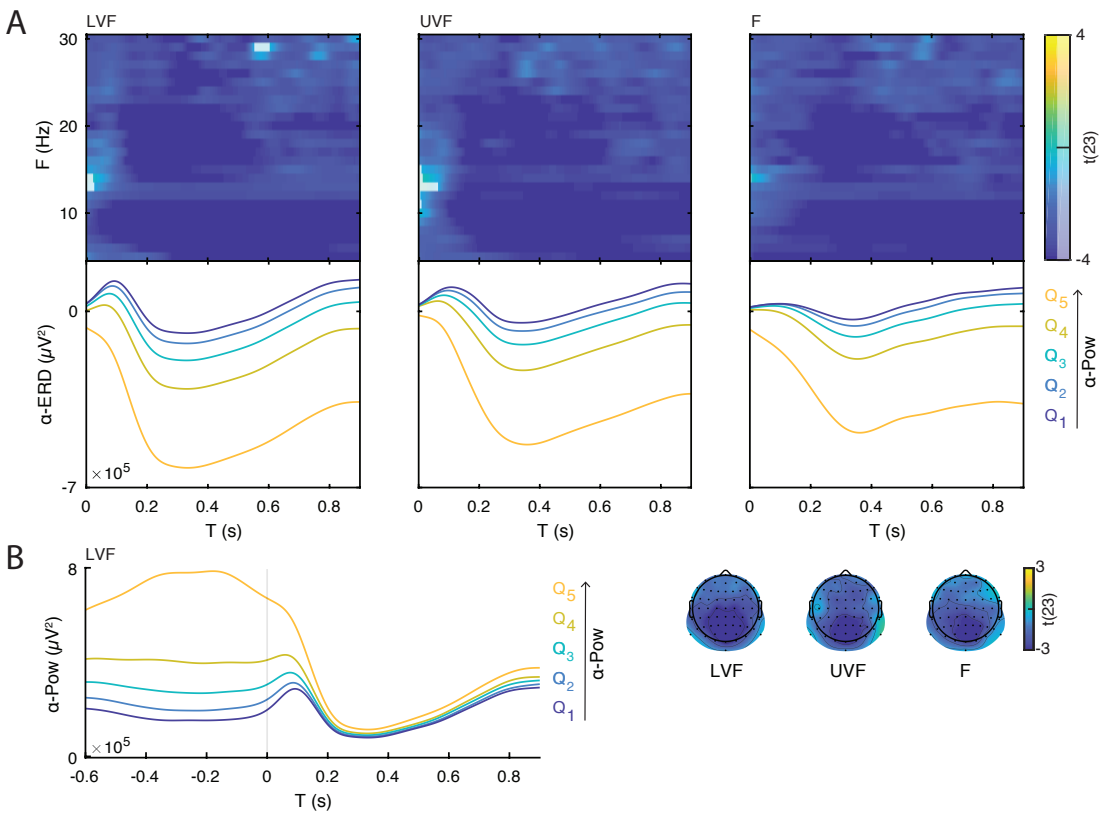

Figure 6: Prestimulus power determines the magnitude of event-related desynchronization (ERD). **A**: Group-level t statistics map of the difference in ERD amplitude between states of weak (Q_1) and strong (Q_5) prestimulus power for lower visual field stimuli (column 1, LVF), upper visual field stimuli (column 2, UVF), and in fixation-only trials (column 3, F). Negative values (blue) indicate that the amplitude of the ERD increases during states of strong prestimulus power. The map is averaged across electrodes of the significant cluster. The maps are masked by a p value of 0.05 using two-sided cluster permutation testing. Note that the x axis refers to post-stimulus ERD time, while the y axis refers to the frequency of prestimulus oscillatory power. Bottom insets: visualization of the normalized ERD time course separately for the 5 bins of prestimulus power (weak to strong: Q_{1-5}, blue to yellow), computed at the electrode and frequency of minimum t-statistics. Time 0 indicates stimulus onset. The topographies show the negative t statistics of the significant clusters averaged for the α-frequency band (8–12 Hz) and for the late time window (0.200–0.900 s), separately for each trial type. Black dots represent electrodes comprising the significant cluster. **B**: Group-average power envelope shown separately for the 5 bins of prestimulus power (weak to strong: Q_{1-5}, blue to yellow) averaged for the α-frequency band and occipital electrodes. These results show that states of strong prestimulus power are followed by strong ERD.

After demonstrating that the late ERP amplitude correlates with the ERD magnitude, and that the ERD magnitude in turn correlates with prestimulus power, we tested whether prestimulus power is directly correlated with the amplitude of the late ERP component. To this end, we compared the late ERP amplitude between groups of trials with weak and strong prestimulus power estimated for each frequency and electrode. For the group-level statistical analysis, we used cluster permutation test to determine significant differences across ERP time points, prestimulus-power frequencies, and electrodes.

The statistical test during the late time window revealed a significant, sustained, and positive cluster in each trial type, indicating that the late ERP component was amplified during states of strong prestimulus power.

In LVF stimulation trials, the significant positive cluster ($p < 0.001$) spanned time points from 0.402 to 0.900 s, frequencies between 5 and 25 Hz, and all 64 electrodes (Fig 3 A/B, column 1). The maximum t statistic was found at 11 Hz, 0.676 s, and at electrode POz.

In UVF stimulation trials, the significant positive cluster ($p = 0.004$) spanned time points from 0.445 to 0.900 s relative to stimulus onset, frequencies between 5 and 15 Hz, and all 64 electrodes (Fig 3 A/B, column 2). The maximum t statistic was found at 5 Hz, 0.648 s, and at electrode CP1.

In F trials, the significant positive cluster ($p < 0.001$) spanned time points from 0.484 to 0.900 s relative to stimulus onset, frequencies between 5 and 23 Hz, and all 64 electrodes (Fig 3 A/B, column 3). The maximum t statistic was found at 7 Hz, 0.781 s, and at electrode POz.

Taken together, these results show that, first, the late ERP component is likely generated by a baseline shift during the ERD of non-zero mean oscillations; second, that states of strong prestimulus power are followed by strong ERD, which manifests as an enhancement of the late ERP component.

Evidence against a confound by sleepiness

To ensure that the relationship between prestimulus power and ERP amplitude was not simply an epiphenomenon of time-varying variables such as sleepiness, we analyzed the scores of a subjective sleepiness questionnaire that participants filled in at the end of every block (Karolinska Sleepiness Scale, KSS: Kaida et al., 2006a,b). First, at the single-subject level, we computed the correlation between prestimulus oscillatory power and KSS rating. At the group-level, we tested whether these correlations were significantly different from 0. We found significant positive clusters for frequencies below 18 Hz and with a widespread topography in each trial type (Fig S1 A; for details see SI). This result indicates that the stronger the prestimulus power, the higher the subjective sleepiness. Within each participant we removed the contribution of sleepiness to the trial-by-trial estimates of oscillatory power and repeated the power-ERP analysis with these corrected power estimates. The results of this re-analysis (Fig S1 B) were virtually identical to the ones obtained with raw power estimates (Fig 3 B), suggesting that the effects we observed are not confounded by sleepiness.

Discussion

Numerous studies have demonstrated that spontaneous fluctuations of prestimulus brain states can account for the trial-by-trial variability in sensory ERP amplitude. Specifically, the power of low-frequency neural oscillations (8–30 Hz) was found to be associated with ERP amplitude in visual, auditory, and somatosensory modality (e.g. Becker et al., 2008; Jones et al., 2009; De Blasio and Barry, 2013; Roberts et al., 2014). However, the results have been mixed: several studies found decreased ERP amplitude during states of strong prestimulus power (Rahn and Başar, 1993; Roberts et al., 2014; Becker et al., 2008; Başar and Stampfer, 1985; Jasiukaitis and Hakerem, 1988); while others studies found increased ERP amplitude during states of strong prestimulus power (Dockree et al., 2007; Becker et al., 2008; Roberts et al., 2014; Başar and Stampfer, 1985; Jasiukaitis and Hakerem, 1988; Barry et al., 2000). Therefore, the precise mechanism by which prestimulus oscillations modulate the neural response to sensory stimuli constitutes a continuing subject of debate in neuroscience. We addressed this issue by considering different mechanisms of ERP generation and how they may depend on prestimulus oscillations: namely, additive and baseline shift mechanisms. First, early ERP components are thought to reflect neural activation in sensory areas adding to ongoing activity. Accordingly, we predicted that early ERP components would be attenuated during states of strong prestimulus low-frequency power, as suggested by

physiological inhibition accounts (Haegens et al., 2011). Second, the late ERP component is likely generated by a post-stimulus modulation of ongoing oscillations (ERD) via baseline shift (Nikulin et al., 2007). Accordingly, we predicted that the late ERP component would be enhanced during states of strong prestimulus power, which are also associated with strong ERD. These predictions were confirmed by the data.

Functional inhibition mechanism

The results on the early ERP components in this study ($<$ 0.200 s: C1/N150) confirm and extend findings from past literature in the visual and auditory modalities. Specifically, previous studies in the visual modality found a negative relationship between prestimulus α-band power and the amplitude of the visual N1P2 (i.e. amplitude difference between N1 and P2 components Rahn and Başar, 1993), N1 (Roberts et al., 2014) and N175 components (Becker et al., 2008). A similar pattern of results was found for the N100 in the auditory modality (Başar and Stampfer, 1985; Jasiukaitis and Hakerem, 1988). It is important to note that previous results (e.g. Başar and Stampfer, 1985; Becker et al., 2008) that have been used to support the functional inhibition account could actually have been caused by a baseline shift. In the current study, we leverage the fact that the C1 has a well-known polarity reversal as a function of the visual field of the stimulus. By showing that the absolute amplitude of the C1 component is diminished by stronger prestimulus power, regardless of polarity, we can rule out a baseline shift which would affect both polarities in the same direction (e.g, a net increase or decrease of voltage). This provides the first conclusive evidence for the functional inhibition effect of prestimulus oscillations on the ERP amplitude.

Unlike in the visual and auditory modality, the relationship between prestimulus power and early ERP components in the somatosensory modality (e.g. N1) may be non-linear (inverted U-shaped: Zhang and Ding, 2009; Ai and Ro, 2014; Forschack et al., 2017) or vary across early components (i.e. negative for M50 and positive for M70, P35 and P60: Jones et al., 2009; Nikouline et al., 2000). Similarly, the relationship between prestimulus power and somatosensory perceptual performance has been found to have an inverted U-shape (Linkenkaer-Hansen et al., 2004), or be linear (Haegens et al., 2011; Craddock et al., 2016). Taken together, these findings suggest that in the somatosensory domain distinct functional mechanisms may map onto low-frequency oscillations.

Importantly, several studies report a positive relationship between prestimulus α-band power and the amplitude of the visual N100 (Jansen and Brandt, 1991; Brandt, 1997), N1P2 (Brandt et al., 1991; Brandt and Jansen, 1991; Barry et al., 2000) and P200 (Jansen and Brandt, 1991). Thus, these studies appear inconsistent with the current results and other studies in the visual and auditory modality. However, a direct comparison is difficult for several reasons. First, some of these studies delivered visual stimuli to participants with eyes closed (Brandt and Jansen, 1991; Brandt et al., 1991; Brandt, 1997; Jansen and Brandt, 1991). Instead, the majority of previous studies (including ours) delivered visual stimuli to participants with eyes open. It is known that oscillatory power in low frequencies has different spectral (Barry et al., 2007) and functional (Kaida et al., 2006a) properties depending on whether subjects' eyes are open or closed: thus, these inconsistencies may be due to the eyes-open/closed difference. Second, unlike our study, which analyzed a broad frequency band, 64 electrodes, and an extensive post-stimulus time window (0–0.900 s), most previous studies only analyzed a narrow frequency band, few electrodes and a single time point. Therefore, it is possible that the inconsistent effects in previous studies might have been due to this selective (and under-sampled) analysis of EEG data. Third, some previous studies lack of: i) sufficient description of the EEG analysis (e.g., Brandt, 1997), ii) adequate statistical power (due to low number of participants or trials: e.g., Brandt et al., 1991; Brandt and Jansen, 1991; Brandt, 1997), and iii) quantitative statistical testing (qualitative reports: e.g.,

Brandt, 1997). Accordingly, these reasons make it difficult to compare these studies to the current one.

The present results have implications for the role of low-frequency oscillations in perceptual decision-making and in the top-down control over sensory processing (e.g., by spatial attention). In fact, numerous studies have found that weak prestimulus α-band power increases observers' hit rates for near-threshold stimuli (Ergenoglu et al., 2004; van Dijk et al., 2008; Chaumon and Busch, 2014). More recently, studies have demonstrated that this effect is not, in fact, due to more accurate perception, but due to a more liberal detection bias (Limbach and Corballis, 2016; Iemi et al., 2017; Craddock et al., 2016; Iemi and Busch, 2018) and a concomitant increase in confidence (Samaha et al., 2017b) and subjective visibility (Benwell et al., 2017b). Unfortunately, conventional signal detection theory cannot be used to distinguish between alternative kinds of bias (Morgan et al., 2013; Witt et al., 2015). Specifically, a change in bias could be due to a change in observer's deliberate decision strategy without any change in sensory processing (decision bias). Alternatively, a change in bias could be due to a change in the subjective appearance of stimuli (perceptual bias): liberal perceptual bias during states of weak prestimulus power could result from increased neural excitability amplifying both neural responses to sensory stimuli (thereby increasing hit rates) and responses to noise (thereby increasing false alarm rates). Interestingly, the present finding that the C1 is amplified during states of weak prestimulus power, indicates that even the earliest visual evoked responses are modulated by prestimulus oscillations. Even though we could not study an equivalent amplification of responses to noise using the present paradigm, this finding supports a perceptual bias mechanism more than a decision bias mechanism.

Furthermore, many experiments have noted a relationship between the topography of α-band power and the focus of covert spatial attention (e.g., Samaha et al., 2016). However considerable debate exists as to whether this preparatory α-band modulation (and hence spatial attention) is capable of modulating feed-foreward visual input (e.g., the C1 component). Our results show a clear impact of spontaneous α and β-band power on C1 amplitudes, supporting the idea that attention-related low-frequency modulation could also amplify very early sensory processing. However, it is possible that attention-related and spontaneous oscillations have different effects on the amplitude of the C1 component. This question is a candidate for future investigation, ideally, by using stimuli such as those employed here, which generated robust C1 responses.

Baseline shift mechanism

In this study we demonstrated that the late component of the visual ERP was generated by an amplitude modulation of non-zero mean oscillations via baseline shift. Note that this mechanism is expected to specifically generate slow ERP components ($<$ 5 Hz), visible during the late time window, because it is not possible to amplitude modulate low-frequency oscillations on faster time scales (Nikulin et al., 2007; Montez et al., 2009).

There are four requirements to demonstrate the baseline shift mechanism. First, the ongoing oscillations must have a non-zero mean. To this end, we first estimated the non-zero-mean property of resting-state oscillations using $AFAI$ and BSI. The analysis of resting-state oscillations revealed that α- and β-band oscillations were characterized by a negative non-zero-mean. The frequencies and electrodes of the significant cluster for $AFAI$ was more extended relative to the cluster for BSI. This could be due to the fact that, unlike BSI, $AFAI$ is biased by harmonics and thus it reflects both non-zero mean oscillations and the "comb-shape" of oscillations which may yield amplitude asymmetries even when the signal has a zero mean (Nikulin et al., 2010a,b). Thus, $AFAI$ is expected to be susceptible to more asymmetry-related features with larger spatial and spectral distribution compared to BSI.

Second, sensory stimuli must modulate the amplitude of ongoing oscillation. To test this requirement, we estimated the power modulation in the post-stimulus window relative to a prestimulus baseline (i.e., event-related oscillations: ERD/ERS). We observed a strong ERD in frequencies between 6 and 30 Hz in all three trial types. In F trials there were no robust early evoked components due to the lack of strong visual input, yet we observed an ERD following the same spatio-temporal dynamics as in stimulation trials (LVF and UVF, though of a lesser magnitude). In addition to the ERD, we also observed a strong ERS below 8 Hz in stimulation trials, but not in F trials, possibly reflecting a leakage from the robust evoked components measured during the early time window.

Third, the non-zero mean and the late ERP must have opposite polarity. Consistent with this requirement, our results showed that oscillations with a negative non-zero mean were associated with a late ERP component of positive polarity. Fourth, ERD magnitude must correlate with the amplitude of the late ERP component. Our results indicated that strong ERD of non-zero mean oscillations was associated with enhanced ERP amplitude during the late time window. Importantly, the late ERP component was characterized by a topography and time-course similar to the ones of the ERD, consistent with Mazaheri and Jensen (2008). Taken together, these findings confirm the four requirements necessary to demonstrate the baseline shift mechanism for the generation of the late ERP component.

A prediction of the baseline shift mechanism is that stronger ERD occurs during states of stronger prestimulus power, which generates a greater baseline shift. In the case of negative non-zero-mean oscillations, this process results in an enhancement of the late ERP component with positive polarity. To test this prediction, we analyzed how prestimulus power affects the ERD magnitude, and in turn the amplitude of the late ERP component. We found a positive relationship between prestimulus power and ERD magnitude, consistent with previous studies (Becker et al., 2008; Tenke et al., 2015; Benwell et al., 2017a). Furthermore, we found a positive relationship between prestimulus power and the amplitude of the late ERP component. These results confirm and extend previous findings in visual and auditory modalities. Specifically, in the visual modality prestimulus α-band power was found to be positively correlated with the ERP amplitude in a late time window starting from 0.200 s relative to stimulus onset (0.550–0.800 s: Dockree et al., 2007; 0.220-0.310 s: Becker et al., 2008; 0.400 s: Roberts et al., 2014). A similar pattern of results was found on late ERP components in the auditory modality (0.250–0.800 s Jasiukaitis and Hakerem, 1988; 0.400 s Başar and Stampfer, 1985; 0.200–0.500 s Barry et al., 2000). Previous studies (e.g. Barry et al., 2000) were unable to explain the positive relationship between α-power and ERP amplitude, which appeared inconsistent with the functional inhibition account (Haegens et al., 2011). This study thus resolves this apparent inconsistency in previous literature, by demonstrating that this positive relationship can be accounted for by the baseline shift mechanism, rather than functional inhibition.

It may seem surprising that the effects of prestimulus power on the late ERP occurred after the peak of the classically-defined slow component at approximately 0.300 s relative to stimulus onset (Nikulin et al., 2007; Mazaheri and Jensen, 2008). While early ERP components are likely generated primarily through the additive mechanism (because ERD is negligible in this time window), late ERP components can have a contribution from both additive and baseline shift mechanisms. Functional inhibition of additive components in the initial part of the late time window might have canceled the amplification effect due to the baseline shift. This cancellation might explain the lack of a significant effect at the peak of the late component. In contrast, the ERP during the later time window ($>$ 0.400 s) is more likely to show primarily baseline shift-generated components and thus is more susceptible to the amplification effect of prestimulus power.

We conclude that the positive modulation of the late ERP component is directly produced by the modulation of ERD magnitude as a function of prestimulus power. This provides the first evidence

that the effect of prestimulus oscillations on the late ERP component is due to the mechanism of baseline shift.

α- and β-band oscillations: a similar functional role?

The results of this study demonstrate a modulatory role of low-frequency oscillations on ERP amplitude. Both effects of prestimulus oscillations on early and late ERP components were characterized by a broad frequency range spanning the α- and β-band. Likewise, the ERD and the non-zero-mean property of oscillations were found for both the α-band and β-band. Specifically, α-band ERD was sustained in time while β-band ERD was more transient, consistent with previous studies (e.g., Salenius et al., 1997). This suggests that β-band ERD may also reflect the generation of late ERP component. One possible explanation for this multi-band effect can be due to the non-sinusoidal nature of neural oscillations (e.g., "comb-shape": Cole and Voytek, 2016), where α- and β-band power covary. In this case the event-related power modulation would similarly affect α- and β-band activity. Because of such comodulaiton, baseline-shifts associated with α-band oscillations would also appear for β-band oscillations, resulting in similar BSI and $AFAI$ for both frequency bands (Nikulin et al., 2010a).

The β-band effect may seem surprising as the majority of past literature is focused solely on the α-band due to its high signal-to-noise ratio compared to other frequencies. However, the broad frequency range of the effects reported in this study is in line with studies reporting a temporal and spatial co-modulation of α- and β-band oscillations (Bastos et al., 2015; Lakatos et al., 2016; Michalareas et al., 2016). It is also consistent with recent studies reporting a similar relationship between α- and β-band prestimulus power, perceptual reports (Benwell et al., 2017b; Iemi et al., 2017; Samaha et al., 2017b,a; Iemi and Busch, 2018) and firing rate (Watson et al., 2018). Accordingly, it has been proposed that β-band oscillations exert an inhibitory function, similar to α-band oscillations (Spitzer and Haegens, 2017; Shin et al., 2017; Kilavik et al., 2013).

Conclusion

This study demonstrates that spontaneous fluctuations of oscillatory brain activity modulate the amplitude of visual ERP via two distinct mechanisms: i) functional inhibition of the early additive ERP components and ii) baseline shift affecting the late ERP component. Therefore, these findings show that neural oscillations have concurrent opposing effects on ERP generation. Distinguishing between these effects is crucial for the understanding of how neural oscillations control the processing of sensory information in the human brain.

Materials and Methods

Participants

Previous studies on the relationship between neural oscillations and ERPs have typically reported samples of 7–19 participants (e.g. Jasiukaitis and Hakerem, 1988; Brandt and Jansen, 1991; Rahn and Başar, 1993; Nikulin et al., 2007; Mazaheri and Jensen, 2008; Becker et al., 2008; Dijk et al., 2010; Rajagovindan and Ding, 2011). To ensure a robust estimate of our neurophysiological effect and account for potential missing data (due to e.g., artifacts), we recruited a larger sample of

27 participants (mean age: 26.33, SEM = 0.616; 14 females; 3 left-handed). All participants had normal or corrected-to-normal vision and no history of neurological disorders. Prior to the experiment, written informed consent was obtained from all participants. All experimental procedures were approved by the ethics committee of the German Psychological Society. Two participants were excluded before EEG preprocessing because of excessive artifacts. One participant was excluded after preprocessing because no C1 component could be detected, unlike the rest of the sample. A total of 24 participants were included in the analysis.

Stimuli and Experimental Design

The experiment was written in MATLAB (RRID:SCR_001622) using the Psychophysics toolbox 3 (RRID:SCR_002881; Brainard, 1997; Pelli, 1997). The experiment included a resting-state session and a stimulation session, lasting approximately 1.5 h including self-paced breaks.

The resting-state session was divided in two recording blocks, each of which lasted 330 s, separated by a short self-paced break. In this session participants were required to keep their eyes open and fixated on a mark located at the center of the screen, to avoid movements and not to think of anything in particular.

In the stimulation session, participants were presented with visual stimuli specifically designed to elicit a robust C1 component of the visual ERP. The C1 is described as the earliest component of the visual ERP with a peak latency between 0.055 and 0.09 s and an occipital topography. The C1 component is regarded as an index of initial afferent activity in primary visual cortex, because of its early latency and polarity reversal with reference to V1 anatomy (Di Russo et al., 2001, 2003).

The stimuli consisted of full-contrast bilateral black-and-white checkerboard wedges. Each wedge corresponded to a radial segment of an annular checkerboard (spatial frequency = 5 cycles per degree) with inner and outer circle of 3 and 10° of eccentricity relative to a central fixation point, respectively. Each wedge covers 3.125% of the area of the annular checkerboard and spans 11.25° of visual angle (Vanegas et al., 2013).

In each stimulation trial, a pair of wedges was presented bilaterally either in the UVF or LVF with equal probability. UVF and LVF stimulus positions were located at polar angles of 25° above and 45° below the horizontal meridian, respectively. These asymmetrical positions for UVF and LVF stimuli ensure a stimulation of primarily lower and upper banks of the calcarine fissure, respectively (Aine et al., 1996; Clark et al., 1995; Di Russo et al., 2001, 2003), resulting in a polarity reversal of scalp potentials. A positive C1 component is obtained by LVF stimulation, while a negative C1 component is obtained by UVF stimulation (Di Russo et al., 2001, 2003).

The stimuli were presented for a duration of 0.100 s (Fu et al., 2010; Ding et al., 2014; Kelly et al., 2008) at full contrast (Hansen et al., 2016; Vanegas et al., 2013) on a gray background that was isoluminant relative to the stimuli's mean luminance. The stimuli were presented at a viewing distance of 52 cm, on a cathode ray tube monitor operated at 100 Hz, situated in a dark, radio-frequency-interference (RFI) shielded room. Throughout the experiment, fixation distance and head alignment were held constant by a chin rest.

For each participant the stimulation session included 810 trials, divided into 9 recording blocks. In each block, 60 trials contained stimuli in either LVF or UVF with equal probability (stimulation trials), while 30 trials were stimulus-absent (fixation-only trials, F). Trial type and stimulation field were randomized across trials within each block. To ensure that the participants maintained the gaze to the center, we included a discrimination task at the central fixation mark, similar to previous studies (Di Russo et al., 2001; Chen et al., 2016). In stimulation trials the central

fixation mark turned into either one of two equally probable targets ($>$ or $<$) during stimulus presentation for a duration of 0.100 s. In F trials, the change of the central fixation mark occurred during a 0.100 s window between 1.8 and 2.4 s relative to trial onset. A proportion of correct discrimination responses of approximately 100% was expected if the gaze was maintained on the central fixation mark. This task also ensured that the participants remained alert throughout the experiment. Trials with incorrect discrimination performance were excluded from EEG analysis. Mean accuracy in the fixation task was 94.85% (SEM = 0.0109) and did not significantly differ between the trials types ($p > 0.05$), indicating that participants were able to maintain central fixation. Incorrect trials were discarded from further analysis (mean = 41.08 ; SEM = 8.6199). On average we analyzed 761.36 (SEM = 9.8239) trials per participant.

After target offset, the fixation mark was restored for a duration of 0.100 s. After this delay, the fixation mark turned into a question mark, which instructed the participants to deliver a response via a button press with their dominant hand. After the button press, the fixation mark was displayed again and a new trial started. The following stimulus presentation or fixation task occurred after a variable delay chosen from a uniform distribution between 1.8 and 2.4 s.

In addition to the fixation task, to further prevent eye movements, all participants were trained prior to EEG recording to maintain fixation on the central mark and their fixation ability was monitored throughout the experiment using the electro-oculogram (EOG). Moreover, we used a shape of the fixation mark specifically designed to maximize stable fixation (Thaler et al., 2013).

To control for an effect of sleepiness on the level of ongoing low-frequency power, we asked participants to report their level of sleepiness at the end of each block during resting-state and stimulation session. We used the Karolinska Sleepiness Scale (KSS) which has been validated as an indicator of objective sleepiness (Kaida et al., 2006a,b). The KSS scale consists of a nine-point Likert-type scale ranging from 1 (extremely alert) to 9 (very sleepy) that represents the sleepiness level during the immediately preceding 5 minutes. The scale was presented on the screen at the end of every block and participants were instructed to report how alert they felt during the immediately preceding block by pressing the corresponding number on the keyboard (1–9). After the button press, participants could take a self-paced break and the following block was initiated by a further button-press.

EEG recording and preprocessing

EEG was recorded with a 64-channel Biosemi ActiveTwo system at a sampling rate of 1024 Hz. Electrodes were placed according to the international 10-10 system (electrode locations can be found on the Biosemi website: https://www.biosemi.com/download/Cap_coords_all.xls). The horizontal and vertical electro-oculograms were recorded by additional electrodes at the lateral canthi of both eyes and below the eyes, respectively. As per the BioSemi system design, the Common Mode Sense (CMS) and Driven Right Leg (DRL) electrodes served as the ground. All scalp electrodes were referenced online to the CMS-DRL ground electrodes during recording. Electrodes impedance were kept below 20 mV. The raw data was recorded with ActiView (version 6.05).

The EEGLAB toolbox version 13, running on MATLAB (R2017b), was used to process and analyze the data (Delorme, 2004). In both resting-state and stimulation session, the data were re-referenced to the mastoids and down-sampled to 256 Hz. In the resting-state session, data were epoched from 0 to 330 s relative to the start of the recording block. In the stimulation session, data were epoched from -1.6 to 1.3 s relative to the onset of the stimulus presentation in stimulation trials or to the onset of the fixation task in F trials. In both sessions, the data were then filtered using an

acausal band-pass filter between 0.25 and 50 Hz. We manually removed gross artifacts such as eye blinks and noisy data segments. In the stimulation session, we discarded entire trials when a blink occurred within a critical 0.5 s time window preceding stimulus onset, to ensure that participants' eyes were open at stimulus onset. Note that "stimulus onset" in F trials refers to the time when a C1-eliciting stimulus would be presented in stimulation trials. Furthermore, we manually selected noisy channels on a trial-by-trial basis for spherical spline interpolation (Perrin et al., 1989). We interpolated on average 8.40 channels (SEM = 0.96) in 34.76 trials (SEM = 6.71). No channels were interpolated in the resting-state session. In both sessions, we transformed the EEG data using independent component analysis (ICA), and then we used SASICA (Semi-Automated Selection of Independent Components of the electroencephalogram for Artifact correction) (Chaumon et al., 2015) to guide the exclusion of IC related to noisy channels and muscular contractions, as well as blinks and eye movements. On average, we removed 7.9 (SEM 0.46) and 7.8 (SEM 0.60) out of 72 ICs in the resting-state and stimulation session, respectively.

Event-related potentials

The aim of this study was to examine the influence of prestimulus oscillatory power on ERP amplitude. We used visual stimuli to specifically elicit a robust C1 component of the visual ERP, which reflects initial afferent activity of the primary visual cortex (Di Russo et al., 2001). For each participant we identified the electrode and time point with peak activity between 0.055 and 0.090 s after stimulus onset (peak C1 activity: Di Russo et al., 2001; Bao et al., 2010), separately for LVF and UVF trials. In F trials, no C1 component of the visual ERP is expected. To quantify the ERP for this trial type and to enable comparison with the stimulation trials, we averaged the EEG data across the subject-specific electrodes with peak C1-activity in the stimulation trials. We baseline corrected the ERP for each trial type using a 0.500 s prestimulus window.

Event-related oscillations

We used time-frequency analysis to obtain a measure of ongoing oscillatory power and to estimate event-related oscillations (ERO). We first computed the stimulus-evoked, phase-locked activity (ERP) by averaging the EEG signal across trials. Then, we subtracted the average ERP from single-trial EEG signal. We applied this procedure separately for LVF, UVF, and F trials. This procedure ensures that the resulting ERO estimate does not contain stimulus-evoked activity (Kalcher and Pfurtscheller, 1995). We applied a wavelet transform (Morlet wavelets, 26 frequencies, frequency range: 5–30 Hz, number of cycles increasing linearly from 3 to 8, time window: -1 – 1.3 s relative to stimulus onset) to the EEG signal. This procedure was performed separately for each electrode and for LVF, UVF, and F trials. We then quantified ERO as follows:

$$ERO = P_{post} - \mu(P_{pre}) \tag{1}$$

where P_{post} is a the time course of post-stimulus oscillatory activity and $\mu(P_{pre})$ is the average ongoing power in a prestimulus window between -0.600 and -0.100 s relative to stimulus onset. This window for baseline correction was chosen based on Mazaheri and Jensen (2008) to circumvent the temporal smearing due to the wavelet convolution. ERO $<$ 0 indicates the presence of an event-related desynchronization (ERD), indicating stimulus-induced power attenuation. ERO $>$ 0 indicates the presence of an event-related synchronization (ERS), indicating stimulus-induced power enhancement. This procedure was performed separately for each frequency, electrode and participant.

Hypothesis testing

In this study, we tested two mechanisms: namely, functional inhibition and baseline shift. Functional inhibition implies that the generation of early, additive ERPs is inhibited if stimulation occurs during a state of strong prestimulus activity. In other words, positive and negative early ERP components are expected to become less positive and less negative, respectively, during states of strong prestimulus power.

The baseline shift mechanism implies that states of strong prestimulus oscillations with a non-zero mean are followed by strong power suppression (ERD), which in turn results in an enhancement of the late ERP component.

Prerequisites of the baseline shift mechanism

Previous studies (Nikulin et al., 2007; Mazaheri and Jensen, 2008) proposed the following prerequisites for linking ERO to ERP generation (baseline shift mechanism): i) the ongoing oscillations must have a non-zero mean; ii) sensory stimuli must modulate ERO magnitude; iii) the non-zero mean and the late ERP component must have opposite polarity; iv) ERO magnitude is associated with the amplitude of the late ERP component.

Estimation of non-zero-mean property of resting-state neural oscillations

The aim of the resting-state session was to estimate the non-zero-mean property of ongoing oscillations, which is known to be a critical requirement for generation of the late ERP via baseline shift (Nikulin et al., 2007; Mazaheri and Jensen, 2008). To this end, we used two analytical methods: namely, the Baseline Shift Index (BSI: Nikulin et al., 2007, 2010a) and the Amplitude Fluctuation Asymmetry Index ($AFAI$: Mazaheri and Jensen, 2008). In each participant, we estimated BSI and $AFAI$ for resting-state oscillations for each electrode and frequency between 5 and 30 Hz.

Following Nikulin et al. (2007), to quantify BSI we first band-pass filtered the EEG signal using a 4th-order Butterworth filter centered at each frequency of interest ± 1 Hz. Then, we extracted oscillatory power using the Hilbert transform. Additionally, we low-pass filtered the EEG signal using a 4th-order Butterworth filter with a 3-Hz cut-off frequency. The baseline shifts are low-frequency components, because the amplitude modulation of 8-30 Hz frequency oscillation can be detected only at frequencies considerably lower than 8 Hz. Thus, the low-frequency components are extracted by low-pass filtering the artifact-cleaned data at 3 Hz, based on previous studies (Nikulin et al., 2007, 2010a). We quantified the BSI as the Spearman correlation coefficient (ρ) between the low-passed EEG signal and the band-passed power, separately at each frequency and electrode. Accordingly, $BSI = 0$ indicates no relationship between oscillatory power and low-passed signal, as expected for zero-mean oscillations. $BSI > 0$ indicate that strong oscillatory power is correlated with an increase of the low-passed signal, as expected for positive-mean oscillations; instead, $BSI < 0$ indicate that strong oscillatory power is correlated with a decrease of the low-passed signal, as expected for negative-mean oscillations.

The amplitude modulation of oscillations with a non-zero mean affects the amplitude of peaks and troughs differently. If the peaks are larger than the troughs relative to the zero line, the ERD will make the electric field go to zero and thus reduce the peaks more strongly than the troughs. It follows that, in this case, any amplitude modulation is expected to produce larger variance

for amplitude values of peaks than troughs. The different modulation of peaks and troughs can be captured by the Amplitude Fluctuation Asymmetry index ($AFAI$). Following Mazaheri and Jensen (2008), to quantify $AFAI$ we first band-pass filtered the EEG signal using a 4th-order Butterworth filter centered at each frequency of interest ± 1 Hz, similarly to BSI computation. Then, we identified the time points of peaks and troughs in the band-passed data. These time points were then used to obtain the signal values of peaks and troughs in the non-band-passed (broadband) signal. We quantified the $AFAI$ as the normalized difference between the variance of the peaks and troughs of the signal as follows:

$$AFAI = \frac{Var(S_p) - Var(S_t)}{Var(S_p) + Var(S_t)} \tag{2}$$

where S_p and S_t refer to the peak and trough values, respectively, estimated in the broadband signal, based on the band-passed signal at a specific frequency.

Accordingly, an $AFAI = 0$ indicates that the peaks and troughs are equally modulated (as for a signal that is symmetric relative to the zero line), as expected for zero-mean oscillations. An $AFAI \neq 0$ indicates amplitude asymmetry: namely, positive values indicate a stronger modulation of the peaks relative to the troughs (i.e. positive amplitude asymmetry or positive mean) and negative values indicate a stronger modulation of the troughs relative to the peaks (i.e. negative amplitude asymmetry or negative mean).

Note that the sign of the BSI and $AFAI$ predicts the polarity of the late ERP component: specifically, if the sign is negative (oscillations with a negative mean) and positive (oscillations with a positive mean), event-related power suppression (ERD) will lead to a positive and negative deflection in the ERP, respectively (Nikulin et al., 2007, 2010a; Mazaheri and Jensen, 2008).

Interaction between event-related potentials and oscillations

To provide evidence that the baseline shift mechanism generates the late ERP component, we analyzed the relationship between ERP and ERO (ERS/ERD) across trials, as proposed by Mazaheri and Jensen (2010). According to the baseline shift mechanism, states of strong ERD should result in an enhanced late ERP component. To this end, we first identified trials with particularly weak and strong ERD, and then tested how these trials differed in the ERP amplitude during the late time window (>0.200 s). Specifically, we computed a trial-by-trial estimate of ERO magnitude at each electrode and frequency, averaged across the post-stimulus time window (0–0.900 s) (see Event-related oscillations). We also computed a trial-by-trial estimate of the late ERP component at the subject-specific C1-peak electrode (see Event-related potentials) ($>$ 0.200 s). We baseline corrected single-trial ERP estimates by subtracting the prestimulus signal baseline averaged across a 0.500 s prestimulus window. Then, for each frequency, and electrode, trials were sorted from weak to strong ERD, divided into 5 bins (Linkenkaer-Hansen et al., 2004; Lange et al., 2012; Baumgarten et al., 2014; Iemi et al., 2017), and the amplitude of the late ERP component was calculated for each bin. The binning was done separately for each trial type (LVF, UVF, and F) and for each participant. Furthermore, to enable a comparison of the late ERP component across bins in each participant, the number of trials in each bin was equated by removing the trials recorded at the end of the experiment. To test the hypothesis, we then compared the amplitude of the late ERP component between strongest and weakest ERO bins (see Statistical Testing for more details).

Influence of prestimulus oscillations on event-related potentials and oscillations

We analyzed how prestimulus oscillatory activity influences ERP and ERO across trials. In this analysis, we identified trials with particularly weak and strong prestimulus oscillations, and then tested how these trials differed in the amplitude of the early and late ERP components and in the ERO magnitude. Specifically, we first computed a trial-by-trial estimate of oscillatory power with a Fast Fourier Transform (FFT) during a 0.500 s prestimulus window for each electrode and frequency. The FFT is advantageous because, unlike wavelet convolution, the results of an FFT computed over the prestimulus period cannot be influenced by signals occurring in the post-stimulus window. We also computed a trial-by-trial estimate of ERP components during the early time window ($<$ 0.200 s) and ERP components during the late time window ($>$ 0.200 s) at the subject-specific electrode of C1 peak activity (see Event-related potentials). We baseline corrected single-trial ERP estimates by subtracting the ERP averaged across a 0.500 s prestimulus window. In addition, we computed a trial-by-trial estimate of the ERO (ERD/ERS) at the subject-specific electrode of C1 peak activity and at each frequency and time point in the post-stimulus time window (0–0.900 s) (see Event-related oscillations). In this analysis, both ERP and ERO were quantified at the subject-specific electrode of C1 peak activity to enable comparison between the effects of prestimulus power on ERP and ERO. Then, for each frequency, and electrode, trials were sorted from weak to strong prestimulus power and divided into 5 bins (Linkenkaer-Hansen et al., 2004; Lange et al., 2012; Baumgarten et al., 2014; Iemi et al., 2017). For each bin we calculated the ERO magnitude and the amplitude of the early and late ERP components. The binning was done separately for each stimulation condition (LVF, UVF, and F) and for each participant. Furthermore, to enable a comparison of ERO and ERP across bins in each participant, the number of trials in each bin was equated by removing the trials recorded at the end of the experiment. We compared the ERO magnitude and the amplitude of the early and late ERP components between bins of strongest and weakest prestimulus power (see Statistical Testing for more details).

Because ongoing oscillatory activity (Kaida et al., 2006a,b; van Dijk et al., 2008; Mathewson et al., 2009; Benwell et al., 2017b, 2018) and ERP amplitude (Megela and Teyler, 1979; Budd et al., 1998; Truccolo et al., 2002; De Munck et al., 2004) may co-vary over the course of an experiment as a function of time-varying variables such as sleepiness, their correlation could be epiphenomenal. To rule this out, we asked participants to report their level of sleepiness at the end of each experimental block using the KSS questionnaire (see Stimuli and Experimental Design for more details; Kaida et al., 2006a). We then estimated how prestimulus power was related to KSS ratings throughout the stimulation session. Specifically, we computed a trial-by-trial estimate of prestimulus power for each electrode and frequency using an FFT on the 0.500 s prestimulus window. We obtained a trial-by-trial estimate of KSS scores by assigning each trial within a block with the KSS score collected at the end of the block. We then used Generalized Linear Modeling (GLM) to predict KSS ratings from prestimulus power at the single-trial level. For each participant and for each electrode and frequency, we fit a regression model of the following form:

$$KSS = \beta_0 + \beta_1 P + \varepsilon \tag{3}$$

where KSS is the subjective sleepiness ratings obtained with the KSS questionnaire, P the prestimulus power at each frequency and electrode, β_1 the estimated correlation coefficient indicating the contribution of P in explaining variability in KSS, and ε the residual errors. To remove the sleepiness-related time-varying changes in ongoing power, we recomputed a trial-by-trial measure of oscillatory power as follows:

$$P_{KSS-c} = P - \beta_1 KSS \tag{4}$$

where P is the original power estimates and β_1 the estimated GLM coefficient reflecting the sleepiness-power relationship. We then repeated the binning analysis on the early and late ERP amplitudes described above, with this new trial-by-trial estimate of power where sleepiness-related time-varying changes were ruled out (P_{KSS-c}). If the relationship between prestimulus power and ERP is not determined by sleepiness affecting both variables, this new binning analysis would replicate the results of the analysis performed on raw power estimates.

Statistical testing

In the resting-state session, within each subject, we first computed the $AFAI$ and BSI at each frequency and electrode. For the group-level statistical inference, we then tested whether the $AFAI$ and BSI were significantly different from 0 across the sample of participants.

In the stimulation session, within each subject, we first computed: i) the difference in the late ERP component between the weakest and strongest ERD bins; ii) the difference in ERP between the weakest and strongest prestimulus power bins (separately for the early and late time window); iii) the difference in ERD between the weakest and strongest prestimulus power bins. For the group-level statistical inference, we computed the t statistics of these differences (ΔV) against the null hypothesis that there was no difference between the bins.

In both sessions, a non-parametric cluster based permutation test was used to determine significant effects while addressing multiple comparisons (Maris and Oostenveld, 2007).

We obtained a distribution of the variables of interest (i.e. $AFAI/BSI$ for resting-state session and ΔV for stimulation session) under the null hypothesis by randomly permuting their signs 1000 times across participants. On each iteration, we tested the resulting variables with a two-tailed t-test against zero and assessed the sum of the t-values within the largest contiguous cluster of significant frequency-electrode (in the resting-state session) or time-frequency-electrode points (in the stimulation session) (cluster p-value $= 0.05$), resulting in a distribution of t-sums expected under the null hypothesis. A final p-value was calculated as the proportion of t-sums under the null hypothesis larger than the sum of t-values within clusters in the observed data. Because: i) the cluster permutation test is based on sampling all time points; and ii) the ERP signal comprise early, fast components and late, slow components having different statistical properties, we decided to test for significant effects separately during the early (< 0.200 s) and late (> 0.200 s) time window. To correct for multiple comparisons due to running the test twice on the same time series, we divided the final permutation p value by 2 (final p-value $= 0.025$, bonferroni corrected) and considered effects significant only if their p values was below this threshold. We performed the statistical test separately for positive and negative clusters as recommended by Maris and Oostenveld (2007) for a two-sided cluster permutation test. We focused the statistical analysis on all electrodes, on frequencies from 5 to 30 Hz and between 0 and 0.9 s relative to stimulus onset.

Supplementary Information

Epiphenomenon of sleepiness?

Previous studies on the relationship between prestimulus brain states and ERP amplitude have typically analyzed how differences in ERP amplitude were related to differences in prestimulus power across trials (e.g. Başar and Stampfer, 1985; Jasiukaitis and Hakerem, 1988; Becker et al.,

2008). This across-trial approach treats individual trials as independent samples and therefore ignores the fact that data are collected in temporal order. This is potentially problematic, because it is known that both oscillatory power and ERP amplitude change over the course of an experiment, possibly due to progressive fatigue and sleepiness (Boksem et al., 2005). Specifically, prestimulus power in the α frequency band is known to increase over the course of an experiment (van Dijk et al., 2008; Mathewson et al., 2009; Benwell et al., 2017b, 2018), suggesting increased inhibition, possibly as consequence of fatigue (Kaida et al., 2006a,b). Likewise, The amplitude of early visual (N1: Boksem et al., 2005) and somatosensory (P60m: Nikouline et al., 2000) ERP components is known to change over the course of the experiment. In other words, since prestimulus power and ERP amplitude both covary across time (e.g., as a function of time-varying variables such as fatigue or sleepiness), their correlation could be epiphenomenal. Therefore, previous studies have tried to exclude that the across-trial correlation between ERP amplitude and power is confounded by fatigue by showing that power is not affected by time-varying temporal variables (e.g. trial number Nikouline et al., 2000).

To address this issue, we collected subjective sleepiness ratings (see Stimuli and Experimental Design for details) at the end of each recording block. Then we used GLM to estimate the correlation between these scores and prestimulus power for each electrode, frequency, and trial type. We used cluster permutation test to determine whether this correlation coefficient (i.e., β) were significantly different from 0 across participants. In all trial types (LVF, UVF, and F), we found that subjective sleepiness was positively correlated with low-frequency power. Specifically, in LVF trials there were two significant positive clusters: the first cluster ($p < 0.001$) spanned frequencies between 5 and 10 Hz in 63 electrodes with a centro-frontal peak (Fig S1 A, column 1, top); the second cluster ($p = 0.024$) spanned frequencies between 13 and 18 Hz in 39 electrodes with a centro-frontal peak (Fig S1 A, column 1, bottom). In UVF trials there was one significant positive cluster ($p = 0.005$) between 5 and 9 Hz and in 64 electrodes with an occipital peak (Fig 1 A, column 2). In F trials there was one significant positive cluster ($p < 0.001$) between 5 and 16 Hz and in 62 electrodes with a central peak (Fig S1 A, column 3). We then removed the contribution of sleepiness from the trial estimates of oscillatory power and repeated the binning analysis with these sleepiness-corrected measures of power (P_{KSS-c}, see Influence of prestimulus oscillations on event-related potentials and oscillations for more details).

The effect of P_{KSS-c} on early and late ERP components (Fig S1 B) was virtually identical to the previous analysis with raw power measures (Fig 3 B). Specifically, in LVF trials, the statistical test during the early time window revealed a significant negative cluster ($p = 0.015$) spanning frequencies between 8 and 26 Hz, time points between 0.043 and 0.121 s, and all 64 electrodes, and a significant positive cluster ($p < 0.001$) spanning frequencies between 5 and 30 Hz, time points between 0.086 and 0.200, and all 64 electrodes. In addition, the statistical test during the late time window revealed one significant positive cluster ($p < 0.001$) spanning frequencies between 5 and 26 Hz, time points between 0.371 and 0.900 s, and all 64 electrodes. In UVF trials, the statistical test during the early time window revealed two significant positive clusters ($p < 0.001$): the first cluster spanned frequencies between 5 and 25 Hz, time points between 0.020 and 0.117, and all 64 electrodes; the second cluster spanned frequencies between 5 and 25 Hz, time points between 0.121 and 0.200 s, and all 64 electrodes. In addition, the statistical test during the late time window revealed one significant positive cluster ($p < 0.008$) spanning frequencies between 5 and 17 Hz, time points between 0.449 and 0.902 s, and 62 electrodes. There was also a near-significant positive cluster ($p = 0.035$) at frequencies between 17 and 25 Hz, time points between 0.590 and 0.900 s, and at 62 electrodes. In F trials, no significant cluster was found during the early time window. Instead, the statistical test during the late time window revealed one significant positive cluster ($p = 0.003$) spanning frequencies between 5 and 22 Hz, time points between 0.559 and 0.900 s, and all 64 electrodes.

Taken together, these results indicate that the relationship between prestimulus power and ERP

amplitude is unlikely to be determined by time-varying effects driven by spontaneous fluctuations of fatigue or sleepiness.

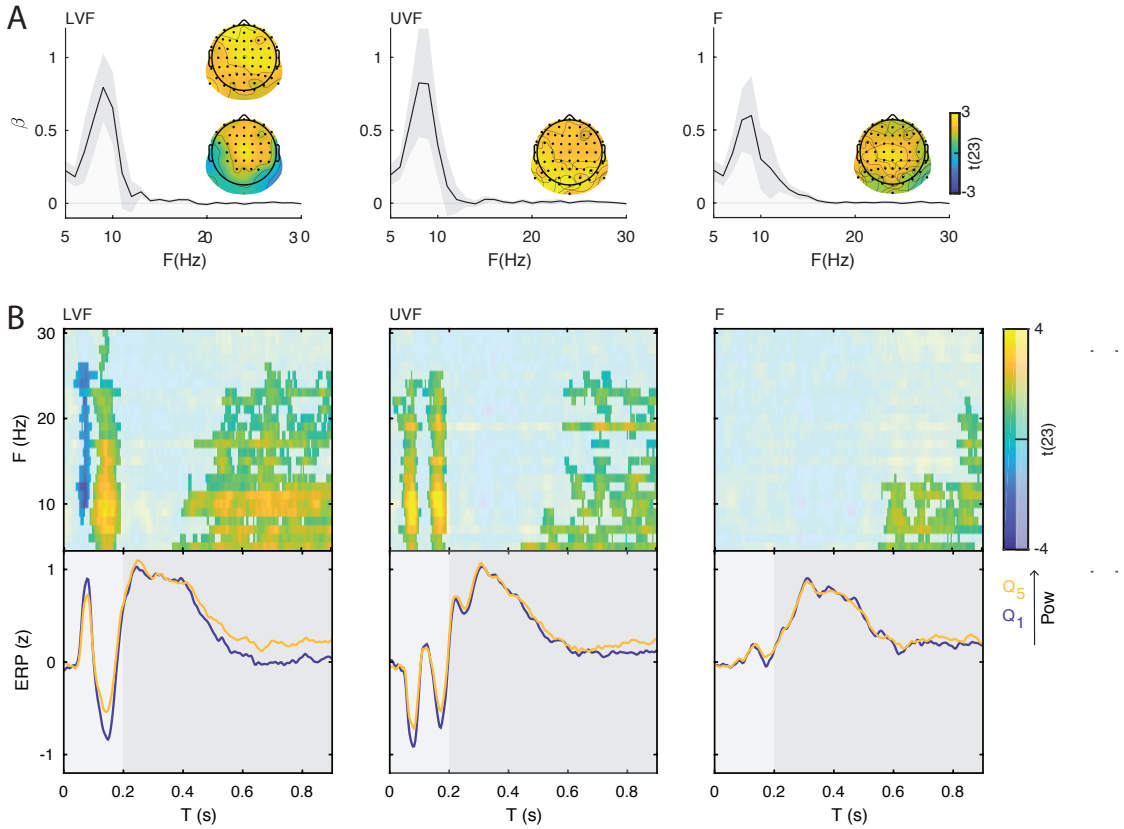

Supplementary Figure 1: Interaction between ER and prestimulus power when sleepiness effects are rules out. **A**: GLM was used to measure the contribution (regression coefficient; GLM β) of oscillatory power to subjective sleepiness ratings, obtained by the KSS questionnaire. The estimated GLM βs were tested against the null hypothesis of no relationship across the sample of participants using cluster permutation test. The plots show the group-level GLM β averaged across respective cluster electrodes, and shown separately for each frequency. Shaded areas indicate $\pm$SEM. The topographies show the positive t statistics of the significant clusters averaged across the respective cluster frequencies. Positive values (yellow) indicate that power is positively correlated with KSS. **B**: Group-level t statistics map of the difference in ERP amplitude between states of weak (Q_1) and strong (Q_5) prestimulus power for lower visual field stimuli (column 1, LVF), upper visual field stimuli (column 2, UVF), and in fixation trials (column 3, F). Positive (yellow) and negative values (blue) indicate that ERP amplitude increases and decreases during states of strong prestimulus power, respectively. The map is averaged across electrodes of the significant cluster. The maps are masked by a p value of 0.025 using separate two-sided cluster permutation testing for early and late ERP time windows. Note that the x axis refers to post-stimulus ERP time, while the y axis refers to the frequency of prestimulus oscillatory power. Bottom insets: visualization of the normalized ERP time course separately for states of strong (Q_5, yellow) and weak (Q_1, blue) prestimulus power. This was computed at the electrode and frequency of minimum/maximum t-statistics during the C1 time window in stimulation trials and during the late time window in F trials. The ERP is characterized by distinct components occurring during the early ($<$ 0.200 s: C1 and N150, light gray) and late time window ($>$ 0.200 s, dark gray). Time 0 indicates stimulus onset. The results replicate the conventional analysis on raw power values reported in the main text. We conclude that the relationship between ERP and prestimulus low-frequency oscillations is unlikely to be determined by time-varying variables such as sleepiness.

References

Ai, L. and Ro, T. (2014). The phase of prestimulus alpha oscillations affects tactile perception. *Journal of neurophysiology*, 111:1300–1307.

Aine, C. J., Supek, S., George, J. S., Lewine, J., Sanders, J., Best, E., Flynn, E. R., and Wood, C. C. (1996). Retinotopic Organization of Human Visual Cortex: Departures from the Classical Model. *Cerebral Cortex*, 6:354–361.

Arieli, A., Sterkin, A., Grinvald, A., and Aertsen, A. (1996). Dynamics of ongoing activity: explanation of the large variability in evoked cortical responses. *Science*, 273(5283):1868–71.

Başar, E. and Stampfer, H. G. (1985). Important Associations Among Eeg- Dynamics , Event-Related Potentials , Short-Term Memory and Learning. *International Journal of Neuroscience*, 26:161–180.

Bao, M., Yang, L., Rios, C., He, B., and Engel, S. A. (2010). Perceptual learning increases the strength of the earliest signals in visual cortex. *Journal of Neuroscience*, 30(45):15080–15084.

Barry, R. J., Clark, A., Johnstone, S., Magee, C., and Rushby, J. (2007). EEG differences between eyes-closed and eyes-open resting conditions. *Clinical Neurophysiology*, 118:2765–2773.

Barry, R. J., Kirkaikul, S., and Hodder, D. (2000). EEG alpha activity and the ERP to target stimuli in an auditory oddball paradigm. *International Journal of Psychophysiology*, 39:39–50.

Bastos, M., Vezoli, J., Kennedy, H., Fries, P., Bastos, M., Vezoli, J., Bosman, C. A., Schoffelen, J.-m., and Oostenveld, R. (2015). Visual Areas Exert Feedforward and Feedback Influences through Distinct Frequency Channels Article Visual Areas Exert Feedforward and Feedback Influences through Distinct Frequency Channels. *Neuron*, pages 390–401.

Baumgarten, T. J., Schnitzler, a., and Lange, J. (2014). Prestimulus Alpha Power Influences Tactile Temporal Perceptual Discrimination and Confidence in Decisions. *Cerebral Cortex*, pages 1–13.

Becker, R., Knock, S., Ritter, P., and Jirsa, V. (2015). Relating Alpha Power and Phase to Population Firing and Hemodynamic Activity Using a Thalamo-cortical Neural Mass Model. *PLOS Computational Biology*, 11(9):e1004352.

Becker, R., Reinacher, M., Freyer, F., Villringer, A., and Ritter, P. (2011). How Ongoing Neuronal Oscillations Account for Evoked fMRI Variability. *Journal of Neuroscience*, 31(30):11016–11027.

Becker, R., Ritter, P., and Villringer, A. (2008). Influence of ongoing alpha rhythm on the visual evoked potential. *NeuroImage*, 39(2):707–716.

Benwell, C. S., London, R. E., Tagliabue, C. F., Veniero, D., Gross, J., Keitel, C., and Thut, G. (2018). Frequency and power of human alpha oscillations drift systematically and independently with time-on-task. *bioRxiv*, page 263103.

Benwell, C. S. Y., Keitel, C., Harvewy, M., Gross, J., and Thut, G. (2017a). Trial-by-trial co-variation of pre-stimulus EEG alpha power and visuospatial bias reflects a mixture of stochastic and deterministic effects. *European Journal of Neuroscience*, pages 1–19.

Benwell, C. S. Y., Tagliabue, C. F., Veniero, D., Cecere, R., Savazzi, S., and Thut, G. (2017b). Prestimulus EEG power preditcs conscious awareness but not objective visual performance. *eNeuro*, 4(6):1–17.

Bijma, F., De Munck, J. C., Huizenga, H. M., and Heethaar, R. M. (2003). A mathematical approach to the temporal stationarity of background noise in MEG/EEG measurements. *NeuroImage*, 20(1):233–243.

Boksem, M. A., Meijman, T. F., and Lorist, M. M. (2005). Effects of mental fatigue on attention: An ERP study. *Cognitive Brain Research*, 25(1):107–116.

Brainard, D. H. (1997). The psychophysics toolbox. *Spatial Vision*, 10(4):433–436.

Brandt, M. E. (1997). Visual and auditory evoked phase resetting of the alpha EEG. *International Journal of Psychophysiology*, 26:285–298.

Brandt, M. E. and Jansen, B. H. (1991). The relationship between prestimulus-alpha amplitude and visual evoked potential amplitude. *The International journal of neuroscience*, 61:261–268.

Brandt, M. E., Jansen, B. H., and Carbonari, J. P. (1991). Pre- spectral EEG patterns and visual evoked response. *Electroencephalogr Clin Neurophysiol*, 80:16–20.

Budd, T. W., Barry, R. J., Gordon, E., Rennie, C., and Michie, P. T. (1998). Decrement of the N1 auditory event-related potential with stimulus repetition: Habituation vs. refractoriness. *International Journal of Psychophysiology*, 31(1):51–68.

Chaumon, M., Bishop, D. V. M., and Busch, N. A. (2015). A Practical Guide to the Selection of Independent Components of the Electroencephalogram for Artifact Correction. *Journal of Neuroscience Methods*, 250:47–63.

Chaumon, M. and Busch, N. (2014). Prestimulus Neural Oscillations Inhibit Visual Perception via Modulation of Response Gain. *Journal of Cognitive Neuroscience*, pages 1–17.

Chen, J., Yu, Q., Zhu, Z., Peng, Y., and Fang, F. (2016). Spatial summation revealed in the earliest visual evoked component C1 and the effect of attention on its linearity. *Journal of Neurophysiology*, 115(1):500–509.

Clark, V., Fan, S., and Hillyard, S. (1995). Identification of early visually evoked potential generators by retinotopic and topographic analysis. *Hum. Brain Mapp.*, 2:170–187.

Cole, S. and Voytek, B. (2016). Brain oscillations and the importance of waveform shape. *Trends in Cognitive Sciences*, xx:1–13.

Craddock, M., Poliakoff, E., El-deredy, W., Klepousniotou, E., and Lloyd, D. M. (2016). Prestimulus alpha oscillations over somatosensory cortex predict tactile misperceptions. *Neuropsychologia*, 96(2017):9–18.

De Blasio, F. M. and Barry, R. J. (2013). Prestimulus delta and theta determinants of ERP responses in the Go/NoGo task. *International Journal of Psychophysiology*, 87(3):279–288.

De Munck, J. C., Bijma, F., Gaura, P., Sieluzycki, C. A., Branco, M. I., and Heethaar, R. M. (2004). A maximum-likelihood estimator for trial-to-trial variations in noisy MEG/EEG data sets. *IEEE Transactions on Biomedical Engineering*, 51(12):2123–2128.

Delorme, A. (2004). Eeglab: an open source toolbox for analysis of single-Trial eeg dynamics including independent component analysis. *Journal of Neuroscience Methods*, 134(1):9–21.

Di Russo, F., Martinez, A., and Hillyard, S. A. (2003). Source analysis of event-related cortical activity during visuo-spatial attention. *Cerebral Cortex*, 13(5):486–499.

Di Russo, F., Martínez, A., Sereno, M. I., Pitzalis, S., and Hillyard, S. A. (2001). Cortical sources of the early components of the visual evoked potential. *Human Brain Mapping*, 15(2):95–111.

Dijk, H. V., Werf, J. V. D., Mazaheri, A., Medendorp, W. P., and Jensen, O. (2010). Modulations in oscillatory activity with amplitude asymmetry can produce cognitively relevant event- related responses. *Proc. Natl. Acad. Sci. U. S. A.*, 107(2):900–905.

Ding, Y., Martinez, A., Qu, Z., and Hillyard, S. A. (2014). Earliest stages of visual cortical processing are not modified by attentional load. *Human Brain Mapping*, 35(7):3008–3024.

Dockree, P. M., Kelly, S. P., Foxe, J. J., Reilly, R. B., and Robertson, I. H. (2007). Optimal sustained attention is linked to the spectral content of background EEG activity: Greater ongoing tonic alpha ($\sim$10 Hz) power supports successful phasic goal activation. *European Journal of Neuroscience*, 25(3):900–907.

Ergenoglu, T., Demiralp, T., Bayraktaroglu, Z., Ergen, M., Beydagi, H., and Uresin, Y. (2004). Alpha rhythm of the eeg modulates visual detection performance in humans. *Cognitive Brain Research*, 20(3):376–383.

Forschack, N., Nierhaus, T., Müller, M. M., and Villringer, A. (2017). Alpha-Band Brain Oscillations Shape the Processing of Perceptible as well as Imperceptible Somatosensory Stimuli during Selective Attention. *The Journal of Neuroscience*, 37(29):6983–6994.

Fu, S., Fedota, J. R., Greenwood, P. M., and Parasuraman, R. (2010). Dissociation of visual C1 and P1 components as a function of attentional load : An event-related potential study. *Biological Psychology*, 85(1):171–178.

Goldman, R. I., Stern, J. M., Englel Jr, J., and Cohen, M. S. (2002). Simultaneous EEG and fMRI of the alpha rhythm. *NeuroReport*, 13(18):2487–2492.

Haegens, S., Nacher, V., Luna, R., Romo, R., and Jensen, O. (2011). α-Oscillations in the monkey sensorimotor network influence discrimination performance by rhythmical inhibition of neuronal spiking. *Proceedings of the National Academy of Sciences of the United States of America*, 108(48):19377–19382.

Hansen, B. C., Haun, A. M., Johnson, A. P., and Ellemberg, D. (2016). On the Differentiation of Foveal and Peripheral Early Visual Evoked Potentials. *Brain Topography*, 29(4):506–514.

Harvey, B. M., Vansteensel, M. J., Ferrier, C. H., Petridou, N., Zuiderbaan, W., Aarnoutse, E. J., Bleichner, M. G., Dijkerman, H. C., van Zandvoort, M. J. E., Leijten, F. S. S., Ramsey, N. F., and Dumoulin, S. O. (2013). Frequency specific spatial interactions in human electrocorticography: V1 alpha oscillations reflect surround suppression. *NeuroImage*, 65:424–432.

Iemi, L. and Busch, N. A. (2018). Moment-to-moment fluctuations in neuronal excitability bias subjective perception rather than strategic decision-making. *eNeuro*, 5(3):1–13.

Iemi, L., Chaumon, M., Crouzet, S. M., and Busch, N. A. (2017). Spontaneous Neural Oscillations Bias Perception by Modulating Baseline Excitability. *Journal of Neuroscience*, 37(4):807–819.

Jansen, B. H. and Brandt, M. E. (1991). The effect of the phase of prestimulus alpha activity on the averaged visual evoked response. *Electroencephalography and Clinical Neurophysiology/ Evoked Potentials*, 80(4):241–250.

Jasiukaitis, P. and Hakerem, G. (1988). The effect of prestimulus alpha sctivity on the P300. *Psychophysiology*, 25:157–165.

Jensen, O. and Mazaheri, A. (2010). Shaping functional architecture by oscillatory alpha activity: gating by inhibition. *Frontiers in human neuroscience*, 4(186):1–8.

Jones, S. R., Pritchett, D. L., Sikora, M. A., Stufflebeam, S. M., Hamalainen, M., and Moore, C. I. (2009). Quantitative Analysis and Biophysically Realistic Neural Modeling of the MEG Mu Rhythm: Rhythmogenesis and Modulation of Sensory-Evoked Responses. *Journal of Neurophysiology*, 102(6):3554–3572.

Kaida, K., Takahashi, M., Åkerstedt, T., Nakata, A., Otsuka, Y., Haratani, T., and Fukasawa, K. (2006a). Validation of the Karolinska sleepiness scale against performance and EEG variables. *Clinical Neurophysiology*, 117(7):1574–1581.

Kaida, K., Takahashi, M., Åkerstedt, T., Nakata, A., Otsuka, Y., Haratani, T., and Fukasawa, K. (2006b). Validation of the Karolinska sleepiness scale against performance and EEG variables. *Clinical Neurophysiology*, 117(7):1574–1581.

Kalcher, J. and Pfurtscheller, G. (1995). Discrimination between phase-locked and non-phase-locked event-related EEG activity. *Electroencephalography and Clinical Neurophysiology*, 94:381–384.

Kelly, S. P., Gomez-Ramirez, M., and Foxe, J. J. (2008). Spatial attention modulates initial afferent activity in human primary visual cortex. *Cerebral Cortex*, 18(11):2629–2636.

Kilavik, B. E., Zaepffel, M., Brovelli, A., MacKay, W. A., and Riehle, A. (2013). The ups and downs of beta oscillations in sensorimotor cortex. *Experimental Neurology*, 245:15–26.

Kraut, M. A., Arezzo, J. C., and Vaughan, H. G. (1985). Intracortical generators of the flash VEP in monkeys. *Electroencephalography and Clinical Neurophysiology/ Evoked Potentials*, 62(4):300–312.

Lakatos, P., Barczak, A., Neymotin, S. A., Mcginnis, T., Ross, D., Javitt, D. C., and Connell, M. N. O. (2016). Global dynamics of selective attention and its lapses in primary auditory cortex. *Nature neuroscience*, 19(12).

Lakatos, P., Chen, C. M., O'Connell, M. N., Mills, A., and Schroeder, C. E. (2007). Neuronal Oscillations and Multisensory Interaction in Primary Auditory Cortex. *Neuron*, 53(2):279–292.

Lange, J., Halacz, J., Van Dijk, H., Kahlbrock, N., and Schnitzler, A. (2012). Fluctuations of prestimulus oscillatory power predict subjective perception of tactile simultaneity. *Cerebral Cortex*, 22(11):2564–2574.

Limbach, K. and Corballis, P. M. (2016). Prestimulus alpha power influences response criterion in a detection task. *Psychophysiology*, 00.

Linkenkaer-Hansen, K., Nikulin, V. V., Palva, S., Ilmoniemi, R. J., and Palva, J. M. (2004). Prestimulus oscillations enhance psychophysical performance in humans. *The Journal of neuroscience*, 24(45):10186–90.

Mäkinen, V., Tiitinen, H., and May, P. (2005). Auditory event-related responses are generated independently of ongoing brain activity. *Neuroimage*, 24:961–968.

Maris, E. and Oostenveld, R. (2007). Nonparametric statistical testing of EEG- and MEG-data. *Journal of Neuroscience Methods*, 164:177–190.

Mathewson, K. E., Gratton, G., Fabiani, M., Beck, D. M., and Ro, T. (2009). To see or not to see: prestimulus alpha phase predicts visual awareness. *Journal of Neuroscience*, 29:2725–2732.

Mathewson, K. E., Lleras, A., Beck, D. M., Fabiani, M., Ro, T., and Gratton, G. (2011). Pulsed Out of Awareness: EEG Alpha Oscillations Represent a Pulsed-Inhibition of Ongoing Cortical Processing. *Frontiers in psychology*, 2:15.

Mayhew, S. D., Ostwald, D., Porcaro, C., and Bagshaw, A. P. (2013). Spontaneous EEG alpha oscillation interacts with positive and negative BOLD responses in the visual-auditory cortices and default-mode network. *NeuroImage*, 76:362–372.

Mazaheri, A. and Jensen, O. (2006). Posterior α activity is not phase-reset by visual stimuli. *Proc. Natl. Acad. Sci. U. S. A.*, 103(8):2948–2952.

Mazaheri, A. and Jensen, O. (2008). Asymmetric Amplitude Modulations of Brain Oscillations Generate Slow Evoked Responses. *Journal of Neuroscience*, 28(31):7781–7787.

Mazaheri, A. and Jensen, O. (2010). Rhythmic pulsing: linking ongoing brain activity with evoked responses. *Frontiers in human neuroscience*, 4(October):177.

Megela, A. L. and Teyler, T. J. (1979). Habituation and the human evoked potential. *Journal of Comparative and Physiological Psychology*, 93(6):1154–1170.

Michalareas, G., Vezoli, J., Pelt, S. V., Schoffelen, J.-m., Kennedy, H., and Fries, P. (2016). Alpha-Beta and Gamma Rhythms Subserve Feedback and Feedforward Influences among Human Visual Cortical Areas. *Neuron*, 89(2):384–397.

Montez, T., Poil, S.-S., Jones, B. F., Manshanden, I., Verbunt, J. P. A., van Dijk, B. W., Brussaard, A. B., van Ooyen, A., Stam, C. J., Scheltens, P., and Linkenkaer-Hansen, K. (2009). Altered temporal correlations in parietal alpha and prefrontal theta oscillations in early-stage Alzheimer disease. *Proceedings of the National Academy of Sciences of the United States of America*, 106(5):1614–1619.

Morgan, M. J., Melmoth, D., and Solomon, J. A. (2013). Linking hypotheses underlying class a and class b methods. *Visual neuroscience*, 30(5-6):197–206.

Nikouline, V. V., Wikström, H., Linkenkaer-Hansen, K., Kesäniemi, M., Ilmoniemi, R. J., and Huttunen, J. (2000). Somatosensory evoked magnetic fields: Relation to pre-stimulus mu rhythm. *Clinical Neurophysiology*, 111(7):1227–1233.

Nikulin, V. V., Linkenkaer-Hansen, K., Nolte, G., and Curio, G. (2010a). Non-zero mean and asymmetry of neuronal oscillations have different implications for evoked responses. *Clinical Neurophysiology*, 121(2):186–193.

Nikulin, V. V., Linkenkaer-Hansen, K., Nolte, G., Lemm, S., Müller, K. R., Ilmoniemi, R. J., and Curio, G. (2007). A novel mechanism for evoked responses in the human brain. *European Journal of Neuroscience*, 25(10):3146–3154.

Nikulin, V. V., Linkenkaer-Hansen, K., Nolte, G., Palva, M. J., and Curio, G. (2010b). Non-zero mean of oscillations as a mechanism for the generation of evoked responses. Reply to "Amplitude asymmetry as a mechanism for the generation of slow evoked responses". *Clinical Neurophysiology*, 121(7):1149–1150.

Pelli, D. G. (1997). The VideoToolbox software for visual psychophysics: transforming numbers into movies. *Spatial Vision*, 10(4):437–442.

Perrin, F., Pernier, J., Bertrand, O., and Echallier, J. F. (1989). Spherical splines for scalp potential and current density mapping. *Electroencephalography and clinical neurophysiology*, 72:184–187.

Rahn, E. and Başar, E. (1993). Enhancement of visual evoked potentials by stimulation during low prestimulus EEG stages. *The International journal of neuroscience*, 72(1-2):123–136.

Rajagovindan, R. and Ding, M. (2011). From prestimulus alpha oscillation to visual-evoked response: an inverted-U function and its attentional modulation. *Journal of cognitive neuroscience*, 23:1379–1394.

Roberts, D. M., Fedota, J. R., Buzzell, G. A., Parasuraman, R., and McDonald, C. G. (2014). Prestimulus oscillations in the alpha band of the EEG are modulated by the difficulty of feature discrimination and predict activation of a sensory discrimination process. *Journal of cognitive neuroscience*, 26(8):1615–1628.

Salenius, S., Schnitzler, A., Salmelin, R., Jousmäki, V., and Hari, R. (1997). Modulation of human cortical rolandic rhythms during natural sensorimotor tasks. *Neuroimage*, 5(3):221–228.

Samaha, J., Gosseries, O., and Postle, B. R. (2017a). Distinct oscillatory frequencies underlie excitability of human occipital and parietal cortex. *The Journal of Neuroscience*, pages 3413–16.

Samaha, J., Iemi, L., and Postle, B. R. (2017b). Prestimulus alpha-band power biases visual discrimination confidence , but not accuracy. *Consciousness and Cognition*.

Samaha, J., Sprague, T. C., and Postle, B. R. (2016). Decoding and reconstructing the focus of spatial attention from the topography of alpha-band oscillations. *Journal of Cognitive Neuroscience*, 28(8):1090–1097.

Schalk, G. (2015). A general framework for dynamic cortical function: the function-through-biased-oscillations (fbo) hypothesis. *Frontiers in Human Neuroscience*, 9:352.

Scheeringa, R., Mazaheri, A., Bojak, I., Norris, D. G., and Kleinschmidt, A. (2011). Modulation of Visually Evoked Cortical fMRI Responses by Phase of Ongoing Occipital Alpha Oscillations. *Journal of Neuroscience*, 31(10):3813–3820.

Schroeder, C. (1998). A spatiotemporal profile of visual system activation revealed by current source density analysis in the awake macaque. *Cerebral Cortex*, 8(7):575–592.

Schroeder, C. E., Steinschneider, M., Javitt, D. C., Tenke, C. E., Givre, S. J., Mehta, A. D., Simpson, G. V., Arezzo, J. C., and Vaughan, H. G. (1995). Localization of ERP generators and identification of underlying neural processes. *Perspecrives of Event-related Potentials Research (EEG Suppl. 44)*, pages 55–75.

Schroeder, C. E., Tenke, C. E., Givre, S. J., Arezzo, J. C., and Vaughan, H. G. (1990). Laminar analysis of bicuculline-induced epileptiform activity in area 17 of the awake macaque. *Brain Research*, 515(1-2):326–330.

Schroeder, C. E., Tenke, C. E., Givre, S. J., Arezzo, J. C., and Vaughan, H. G. (1991). Striate cortical contribution to the surface-recorded pattern-reversal vep in the alert monkey. *Vision Research*, 31(7-8):1143–1157.

Shah, A. S., Bressler, S. L., Knuth, K. H., Ding, M., Mehta, A. D., Ulbert, I., and Schroeder, C. E. (2004). Neural Dynamics and the Fundamental Mechanisms of Event-related Brain Potentials. *Cerebral Cortex*, 14(5):476–483.

Shin, H., Law, R., Tsutsui, S., Moore, C. I., and Jones, S. R. (2017). The rate of transient beta frequency events predicts behavior across tasks and species. *eLife*, pages 1–31.

Spaak, E., Bonnefond, M., Maier, A., Leopold, A. D., and Jensen, O. (2012). Layer-specific entrainment of gamma-band neural activity by the alpha rhythm in monkey visual cortex. *Current Biology*, 22(24):2313–2318.

Spitzer, B. and Haegens, S. (2017). Beyond the Status Quo : A Role for Beta Oscillations in Endogenous Content (Re) Activation. *eNeuro*, 4(August).

Tenke, C. E., Kayser, J., Abraham, K., Alvarenga, J. E., and Bruder, G. E. (2015). Posterior EEG alpha at rest and during task performance: Comparison of current source density and field potential measures. *International Journal of Psychophysiology*, 97(3):299–309.

Thaler, L., Schütz, A. C., Goodale, M. A., and Gegenfurtner, K. R. (2013). What is the best fixation target ? The effect of target shape on stability of fixational eye movements. *Vision Research*, 76:31–42.

Truccolo, W. A., Ding, M., Knuth, K. H., Nakamura, R., and Bressler, S. L. (2002). Trial-to-trial variability of cortical evoked responses: Implications for the analysis of functional connectivity. *Clinical Neurophysiology*, 113(2):206–226.

van Dijk, H., Schoffelen, J.-M., Oostenveld, R., and Jensen, O. (2008). Prestimulus oscillatory activity in the alpha band predicts visual discrimination ability. *The Journal of neuroscience*, 28(8):1816–1823.

van Kerkoerle, T., Self, M. W., Dagnino, B., Gariel-Mathis, M.-A., Poort, J., van der Togt, C., and Roelfsema, P. R. (2014). Alpha and gamma oscillations characterize feedback and feedforward processing in monkey visual cortex. *Proceedings of the National Academy of Sciences of the United States of America*, 111(40):14332–14341.

Vanegas, M. I., Blangero, A., and Kelly, S. P. (2013). Exploiting individual primary visual cortex geometry to boost steady state visual evoked potentials. *J. Neural Eng*, 109(10):36003–9.

Watson, B. O., Mingxin, D., and Buzsáki, G. (2018). Temporal coupling of field potentials and action potentials in the neocortex. *European Journal of Neuroscience*, pages 1–16.

Witt, J. K., Taylor, J. E. T., Sugovic, M., and Wixted, J. T. (2015). Signal detection measures cannot distinguish perceptual biases from response biases. *Perception*, 44(3):289–300.

Zhang, Y. and Ding, M. (2009). Detection of a Weak Somatosensory Stimulus: Role of the Prestimulus Mu Rhythm and Its Top-Down Modulation. *Journal of Cognitive Neuroscience*, 22(2):307–322.